Радиофизика и радиоастрономия, 1996, т.1, № 1, 70-93

Chaotic Dynamics of Weakly Nonlinear Systems

D.M.Vavriv

Radio Astronomy Institute of the Ukrainian Academy of Sciences
4 Chervonopraporna Street, 310002 Kharkov, Ukraine

The progress made in recent years in the study of chaotic states of weakly nonlinear systems is reviewed. We concern with the class of chaotic states pertaining to physical systems with any degree of nonlinearity however small. The conditions for, and the mechanisms of, the transition to chaos are discussed for the weakly nonlinear oscillators and compared with that for the strongly nonlinear ones. Considerable attention is given to analytical methods of the chaos onset prediction. The dynamics of parametric amplifiers, SQUIDs, and variable stars is considered to illustrate these results.

1. Introduction

It has recently been realized that the chaotic states are typical not only for strongly nonlinear systems, but they can arise in weakly nonlinear dissipative systems as well [1-6]. A wide range of typical situations was found where the chaotic states arise under the weakly nonlinear excitation conditions, including various types of oscillators with a quasi periodic forcing, multimode autonomous and non autonomous systems, distributed systems. The existence of the chaotic states in the quasilinear limit implies that the condition for the chaos to arise is not very stringent for many practical situations, and that the influence of the chaotic instabilities on the dynamics of real systems can be much more severe as compared with the recent thinking.

The main results in this direction of research have been obtained for the systems described by the equations of motion of single or coupled oscillators

$$\ddot{x}_i + \omega_i^2 x_i = \varepsilon F_i(t, x_1, \dot{x}_1, x_2, \dot{x}_2, \ldots x_N, \dot{x}_N),$$
$$i = 1,2,\ldots,N,$$

where x_i are the generalized coordinates of the oscillators, ω_i are their proper frequencies, F_i are the functions describing nonlinearity and dissipation, ε is the parameter of nonlinearity, being small for the weakly nonlinear systems, N is the number of interacting modes. It is well known that this mathematical model naturally arises when studying the dynamics of a variety of systems with a weak nonlinearity.

The chaotic states of weakly nonlinear oscillators manifest themselves in the form of a weak chaotic modulation of the amplitude and phase of a periodic or quasiperiodic oscillation having the frequencies close to the natural frequencies of the oscillators. The characteristic time scale of the modulation is ω_i/ε, which is much greater as compared with $1/\omega_i$. Due to that, the direct numerical study of these states by using the initial system of equations leads to a cumbersome computational procedure. The are also no analytical methods which can be used to detect the chaotic states in this case. Moreover, the weakly nonlinear systems are characterized by specific mechanisms of the transition to chaos as compared with strongly nonlinear systems. Due to these reasons, a demand arose for adequate methods of studying of the weakly nonlinear systems . A large experience thus far is accumulated in this direction, and the investigations of the chaotic dynamics of the weakly nonlinear systems constitute now a separate direction of the research in the field of chaos being important both for the basic study and applications.

In this paper some general approaches to the study of chaotic phenomena in weakly nonlinear systems are described along with the results of the investigations of some practical systems. For better illustration of the obtained results, at first, we review in Section 2 the conditions of the formation of chaotic states in the strongly nonlinear oscillators, and then we compare this process with that going on in the quasilinear limit. When studying the chaotic dynamics of the weakly nonlinear oscillators, we introduce the concept of induced saddle states [7] which appears to be useful for the understanding of the mechanism of the chaos onset. Then we describe several analytical approaches to the chaos onset prediction by using the quasiperiodically forced Duffing-type oscillator as an example. In Section 3 characteristic features of the dynamics of parametrically forced oscillators are considered. The mechanisms of the transition to chaos are discussed along with the conditions of the arising of multistable states. These findings are applied to the stability analysis

of parametric amplifiers. In Section 4 we study conditions for chaos due to the interaction of low- and high-frequency oscillations. The SQUIDs stability is considered to illustrate the significant influence of this effect on the dynamics of some practical systems. Section 5 deals with the chaotic dynamics of multimode systems. We restrict ourselves to a few examples of the two mode systems among a great number of multimode system that have been studied to date. The dynamics of variable stars is discussed here as a recent example of the application of the theory of the weakly nonlinear systems.

2. Conditions for chaos in strongly and weakly nonlinear systems

In this part of the paper we discuss the main differences in mechanisms of the transition to chaos in strongly and weakly nonlinear oscillators. To illustrate these results, we start from the simplest model, as the quasiperiodically forced Duffing-type oscillator

$$\ddot{x}+\omega_0^2 x=\varepsilon\left[-\left(\delta_0+\delta_1 x^2\right)\dot{x}+\gamma x^3+\right.$$
$$\left.+A_1\cos\omega_1 t+A_2\cos\omega_2 t\right] \tag{2.1}$$

Here x is a generalized coordinate of the oscillator, $\delta_0>0$ and $\delta_1>0$ are the coefficients of linear and nonlinear damping, γ is the nonlinearity parameter, ω_0 is the proper frequency of the oscillator, A_1 and A_2 are the amplitudes of the parametric and external forcing with the incommensurate frequencies ω_1 and ω_2. The ε-factor is introduced in eq.(2.1) in order to express in the explicit form the degree of nonlinearity of the oscillator.

Note that the oscillator (2.1) can be considered as the Duffing type oscillator due to the limitations imposed on the coefficients: $\delta_0>0$ and $\delta_1>0$. The case of $\delta_0<0$ and $\delta_1>0$ corresponds to the Van der Pol oscillator, and is not considered here. The interested reader may refer to Refs. [8-10] for the later case.

A great deal of work has already been done to study chaotic solutions of this equation and its special cases. One of such cases is the harmonically forced Duffing oscillator, whose chaotic dynamics has been much investigated starting from the initial works in the field of chaos [11-13]. It was shown that the chaotic motion arises because of the formation of a homoclinic structure in the phase space of the system due to the transverse intersections between the stable and unstable manifolds of hyperbolic periodic orbits. The next important conclusion was made that a strong nonlinearity is required for the chaos onset in any single-degree-of-freedom dissipative oscillator with periodic excitation. The dynamics of the strongly nonlinear oscillator with quasiperiodic forcing was studied, for example, in Refs. [14,15]. Notice that beginning with the above-mentioned paper and up to now, the systems possessing a homoclinic loop (or loops) to a saddle point(s) in their Hamiltonian limit have been mainly considered. With respect to the equation under consideration such saddle points exist in the unperturbed oscillator with $\gamma>0$ when the dissipation and the amplitudes of the external forcing are equal zero. We call this type of singular points as *original saddle points*. The systems with an original saddle point are amenable to a theoretical treatment by using a global perturbation technique developed by Melnikov [11], and that is possibly the main reason why these systems have received much consideration (see Refs.[16,17]). This technique was generalized by Wiggins [18] to quasiperiodically forced oscillators. In the later case, the chaos origin was associated once again with the existence of the original saddle point, and chaotic states of the strongly nonlinear oscillators were considered as for the harmonically forced ones.

However, in the case of quasiperiodically forced oscillators, there is also another way of the chaos arising that is not related with the existence of homoclinic orbits in the unperturbed oscillators, and where the strong nonlinearity of the oscillators is not required. This possibility was predicted and studied independently by several authors in Refs.[1,2,4] and proved experimentally in Refs.[10,11]. The alternative way of the transition to chaos is associated with the occurrence of new saddle orbits in the phase space of the systems under the action of one of the external harmonic component. We call such orbits as *the induced saddle orbits* [7]. With the availability of an additional incommensurate spectral component of low intensity in the external force, a normally hyperbolic invariant tori are formed in the phase space instead of saddle orbits. The chaos results from the transverse intersection between the stable and unstable manifolds of the torus when the perturbation is increased. The formation of a homoclinic structure occurs here at much more lower values of amplitudes of the perturbation as compared to the case when this structure is formed on the base of an original saddle point. Now let us consider in more details these two mechanisms of the chaos

onset, beginning from the case of the strongly nonlinear oscillator.

2.1. Strongly nonlinear oscillators

Let us rewrite eq.(2.1) as a system of first-order equations:

$$\dot{x} = y$$
$$\dot{y} = -\omega_0^2 x + \varepsilon f(x,y,t), \qquad (2.2)$$

where:

$$f(x,y,t) = -(\delta_0 + \delta_1 x^2)\dot{x} + \gamma x^3 + A_1 \cos(\omega_1 t) + A_2 \cos(\omega_2 t) \qquad (2.3)$$

To obtain analytical conditions of the onset of chaos through Melnikov's method, we make use of the fact that at $\delta_0=\delta_1=A_1=A_2=0$ the system under investigation is described by the following Hamiltonian [2]

$$H(x,y) = \frac{y^2}{2} + \frac{\omega_0^2 x^2}{2} - \frac{\varepsilon\gamma x^4}{4}. \qquad (2.4)$$

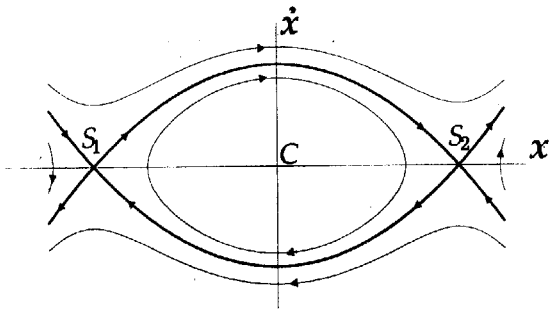

Fig.1. *The phase portrait for the Hamiltonian system (2.4), S_1 and S_2 are saddle points, C is center.*

Provided that $\gamma>0$, this system possesses an original saddle points in the phase space (x,y) with the coordinates

$$y = 0,\ x = \pm\omega_0/\sqrt{\varepsilon\gamma} \qquad (2.5)$$

and a heteroclinic orbit (separatrix loop) shown in fig. 1. Note that a center-type singular point is located at $y=0$, $x=0$ in the phase space of the system (2.4).

The influence of the other terms of the function (2.3) not included in eq.(2.4) is considered as perturbations. It permits to apply the standard Melnikov technique developed for similar systems (see Refs.[1-3] for details). We eventually come to the following condition of the homoclinic structure formation [7]:

$$A_1\omega_1 \operatorname{cosech}\left(\frac{\pi\omega_1}{\sqrt{2}\omega_0}\right) + A_2\omega_2 \operatorname{cosech}\left(\frac{\pi\omega_2}{\sqrt{2}\omega_0}\right) \geq \geq \left|\frac{2\omega_0^3}{3\pi\sqrt{\varepsilon\gamma}}\left(\delta_0 + \frac{\delta_1\omega_0^2}{5\varepsilon\gamma}\right)\right| \qquad (2.6)$$

This criterion is considered as a necessary condition for the chaos to arise. It incorporates a variety of particular cases that have been described up to now in the literature. For example, assuming $\delta_1=0$, we have from eq.(2.6) the condition of a homoclinic structure arising obtained in Ref.[2] for the oscillator with the two-frequency excitation. Setting in addition $A_2=0$ in eq.(2.6), we come to the result given in Ref.[1] for the harmonically forced oscillator.

It is evident from eq.(2.6) that the chaotic oscillations can arise when the oscillator is excited only periodically. Under the quasiperiodic excitation, the threshold for chaos to arise is not changed essentially. Now let us consider the transition to the case of the quasilinear oscillator that corresponds to the limit: $\varepsilon\to 0$. According to the expression (2.5), the manifolds cease to intersect for any values of A_1 and A_2 if the ε-value is sufficiently small. Due to it, this mechanism of the homoclinic structure formation can not lead to the chaos onset in the weakly nonlinear systems.

However, this result is true only when we deal with the formation of homoclinic structures associated with the original saddle points (2.5). The situation is changed dramatically if we take into account that additional saddle states can arise under the action of the external force. In the later case other homoclinic structures can arise on the base of homoclinic loops associated with this states due to the frequencies' interaction of the external forcing. It leads to the chaotic states formation in the weakly nonlinear limit. Thus, to predict analytically the chaos onset in the weakly nonlinear systems, one should at first detect the induced saddle states. In the case under consideration such states are saddle orbits arising under the action of one or each of the harmonic components of the external forcing due to resonances occurring in the system. The direct application of the initial equations (2.1) or (2.2) do not allow detect analytically these orbits as well as to predict the chaos arising. One way around this problem is application of the averaging method [21], and it is demonstrated in the next section.

2.2. Induced saddle states

Let us apply the method of averaging to the system (2.2), assuming that the right-hand side of eq.(2.2) is small, that is, $\varepsilon|f(x,y,t)| << 1$ We are interesting in the case of the resonant excitation of the oscillator, when

$$|\omega_1 - \omega_0| = O(\varepsilon\omega_0), \text{ and } |\omega_2 - \omega_0| = O(\varepsilon\omega_0) \quad (2.7)$$

Then, by using the transformation

$$x = U\cos(\omega_1 t) + V\sin(\omega_1 t)$$
$$y = -U\omega_1\sin(\omega_1 t) + V\omega_1\cos(\omega_1 t) \quad (2.8)$$

and applying the standard averaging procedure, we come to the following system of averaging equations for the slowly varying time functions $U(\tau), V(\tau)$:

$$\frac{dU}{d\tau} = -\left[\alpha_0 + \alpha_1\left(U^2+V^2\right)\right]U - \left[\Delta + \beta\left(U^2+V^2\right)\right]V - p_2\sin\Omega\tau$$
$$\frac{dV}{d\tau} = -\left[\alpha_0 + \alpha_1\left(U^2+V^2\right)\right]V + \left[\Delta + \beta\left(U^2+V^2\right)\right]U - p_1 + p_2\cos\Omega\tau \quad (2.9)$$

where dimensionless parameters are introduced: $\tau = \varepsilon\omega_1 t$, $\alpha_0 = \delta_0/(2\omega_1)$, $\alpha_1 = \delta_1/(8\omega_1)$, $p_1 = A_1/(2\omega_1^2)$, $p_2 = A_2/(2\omega_1^2)$, $\Delta = (\omega_1 - \omega_0)/(\varepsilon\omega_1)$, $\Omega = (\omega_1 - \omega_2)/(\varepsilon\omega_1)$, and $\beta = 3\gamma/(8\omega_1^2) > 0$

For the case of the pure periodic excitation (p_2=0) this system is reduced to a second order autonomous system. On this basis we conclude again that the weakly nonlinear oscillators with harmonic excitation can not have any chaotic states. Such states can arise here only due to the interaction of the external frequencies provided that one of the frequencies induces a saddle orbit in the phase space of the system (2.9).

The transition from the original equation to the averaged ones allows to reduce the investigation of bifurcations of two-dimensional tori in the phase space of the original system (2.1) to the analysis of bifurcations of periodical orbits in the phase space of the system (2.9). It is important to note that the latter system does not contain ε as independent parameter. The ε changes lead only to the variation of the time scale of the excited oscillations, provided that values of the parameters Δ and Ω are kept constant. From this follows that, if the system (2.9) demonstrates chaotic behavior, than such behavior can arise for any degree of ε however small, i.e., in the quasilinear limit.

The averaged equations are convenient tool for the detection of the induced saddle orbits of the initial equation (2.1). In terms of the averaged equations these orbits are seen as saddle singular points. They can be induced by any of the external frequency components, or due to their combined action. We shall consider the case when the amplitude of one of the component, say p_2, is relatively small and the induced saddle states can arise mainly due to the second component. Assuming that p_2=0 and the dissipation is absent, we have instead of (2.9) the following Hamiltonian system:

$$\frac{dU}{d\tau} = -\left[\Delta + \beta\left(U^2+V^2\right)\right]V$$
$$\frac{dV}{d\tau} = \left[\Delta + \beta\left(U^2+V^2\right)\right]U - p_1 \quad (2.10)$$

with Hamiltonian energy given by

$$H(U,V) = \frac{\beta}{4}\left(U^2+V^2\right)^2 + \frac{\Delta}{2}\left[V^2+U^2\right] - p_1 U \quad (2.11)$$

Unlike the previous case (see eq.(2.4)), this Hamiltonian contains the amplitude of the external force p_1 as a parameter. As long as p_1=0, there is only a center-type singular point in the origin of the coordinate, thus, we come to the result following from the Hamiltonian (2.4). For $p_1 \neq 0$ and $-\Delta/\beta > 0$, the center is split into three singular points: two centers and a saddle. This situation is illustrated by the phase portrait of the system (2.11) in fig.2. Note that the phase portrait is characterized by the existence of a double homoclinic orbit (separatrix) going out and in the saddle point with the coordinates $U = U_s$, $V = 0$. Here U_s is the minimum of the real roots of the following cubic equation,

$$U_s^3 + \frac{\Delta}{\beta}U_s - \frac{f}{4} = 0, \quad (2.12)$$

where $f = 4p_1/\beta$.

The separatrix equation was found in ref. [22] and can be written in the form:

$$U_t(\tau') = U_s + S(\tau')\left[2\left(\delta - U_s^2\right) + S(\tau')\right]/f, \quad (2.13)$$

where $S(\tau') = (q^2 - b^2)/(2(q\cosh\tau' - b))$; $\tau' = \beta\mu(\tau - \tau_0)$; $q = \pm 2\sqrt{-2fU_s}$; $b = -4(\delta - U_s^2)$; $\mu^2 = -2fU_s - b^2/4$, $\delta = -\Delta/\beta$, τ_0 is an initial moment of the "slow" time. The signs "+" and "-" correspond to the small and large loops of the separatrix, accordingly.

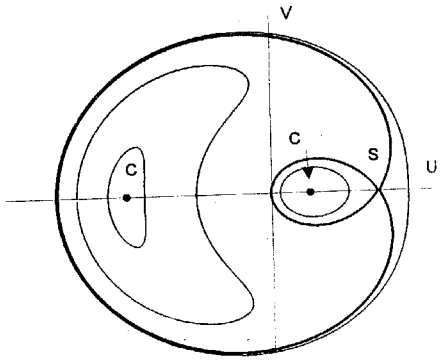

Fig. 2. *Phase portrait of the system (2.11)*

The regions in the parameter space where the saddle states exist are reduced under the influence of dissipation. Let us consider this effect by introducing into the consideration the corresponding dissipative terms into the system (2.10). Then instead of it, we have:

$$\frac{dU}{d\tau} = -\left[\alpha_0 + \alpha_1(U^2+V^2)\right]U - \left[\Delta + \beta(U^2+V^2)\right]V, \tag{2.14}$$

$$\frac{dV}{d\tau} = -\left[\alpha_0 + \alpha_1(U^2+V^2)\right]V + \left[\Delta + \beta(U^2+V^2)\right]U - p_1$$

By means of the stability analysis it can be shown that this system has a saddle point in its phase space when the following conditions are hold:

$$p_1^2 > p_{cr}^2 \equiv \frac{8\alpha_0^3(\alpha_1^2+\beta^2)}{3\sqrt{3}(\beta - \sqrt{3}\alpha_1)^3} \tag{2.15}$$

$$\Delta < \Delta_{cr} \equiv -\alpha_0 \frac{\alpha_1 + \sqrt{3}\beta}{\beta - \sqrt{3}\alpha_1} \tag{2.16}$$

$$\beta > \sqrt{3}\alpha_1 \tag{2.17}$$

When the value of the parameter of nonlinear dissipation α_1 is negligibly small, these conditions read

$$p_1^2 > p_{cr}^2 \equiv \frac{8\alpha_0^3}{3\sqrt{3}\beta} \tag{2.18a}$$

$$\Delta < \Delta_{cr} \equiv -\sqrt{3}\alpha_0 \tag{2.18b}$$

The above given conditions determine the regions in the parameter space where the induced saddle states arise and due to it, they can be considered as necessary conditions for the chaos onset in the weakly nonlinear systems.

We complete these conditions in the following section by using several analytical approaches to the chaos onset study.

2.3. Analytical methods of the chaos onset prediction

2.3.1. Melnikov's criterion.

In practice, Melnikov's method [11] is widely used as the constructive analytic approach to determining the approximate conditions for strange attractors to occur. It is usually applied to dynamical systems of the following form

$$\dot{x} = f(x) + \varepsilon g(x,t), \quad x \in R^n$$

in which a closed homoclinic loop exists when $\varepsilon=0$ (ε is a small parameter). Experience in using Melnikov's method shows that systems which are Hamiltonian when $\varepsilon=0$ are mainly amenable to investigation, although such a constraint is not imposed in the method itself. The main difficulties in the case when the unperturbed system is dissipative arise in determining the position of the homoclinic loop and the determining the solution on it.

Let us apply Melnikov's method to the averaged equations (2.9) to find necessary conditions for the chaos onset with respect to the parameters of the second external spectral component. We make use of the fact that when dissipation and the amplitude of the second external periodic component are equal zero this system becomes Hamiltonian one with the motion equations (2.10) and Hamiltonian energy given by (2.11). The system (2.10) is considered as the unperturbed one. Considering in the system (2.9) the terms with dissipation and the amplitude of this component are small perturbation, we write down the Melnikov function $\Delta_M(\tau_0)$ which determines the distance between the stable and unstable manifolds of the saddle point in the Poincare map of the averaged equations:

$$\Delta_M(\tau_0) = \int_{-\infty}^{\infty} \left[R_1(U_l, V_l, \tau) \cdot Q_0(U_l, V_l) - Q_1(U_l, V_l, \tau) \cdot R_0(U_l, V_l) \right] d\tau \quad (2.19)$$

where

$$R_0 = -\left[\Delta + \beta\left(U_l^2 + V_l^2\right)\right] V_l,$$

$$Q_0 = \left[\Delta + \beta\left(U_l^2 + V_l^2\right)\right] U_l - p,$$

$$R_1 = -\left[\alpha_0 + \alpha_1\left(U_l^2 + V_l^2\right)\right] U_l - p_2 \sin(\Omega\tau),$$

$$Q_1 = -\left[\alpha_0 + \alpha_1\left(U_l^2 + V_l^2\right)\right] V_l + p_2 \cos(\Omega\tau).$$

The functions $U_l(\tau)$ and $V_l(\tau)$ are given by the relations (2.11)-(2.13). After performing the integration in eq.(2.19), one can find from the condition of the manifolds intersections $\Delta_M(\tau_0) = 0$ the following necessary condition of the chaos onset [22, 23]:

$$\frac{p_2}{\alpha_0} \geq \left| \frac{f \sinh(\pi\sigma)}{2\pi\mu^2\sigma^2 \exp\left(-\sigma \cdot \operatorname{sign} q \cdot \arccos(-b\ q)\right)} \right| \times \left\{ 3\mu - 8\delta \arctan\frac{q+b}{2\mu} + \frac{\alpha_1}{\alpha_0}\left[7\delta\mu + \left(8\delta\left(U_s^2 - 2\delta\right) - \frac{3}{4}q^2 \right) \arctan\frac{q+b}{2\mu} \right] \right\}, \quad (2.20)$$

where $\sigma = (2\Omega)/(\beta\mu)$. The equality sign corresponds to $p = p_{cr}$, where p_{cr} is the lowest threshold of the chaotic motion arising with respect to the amplitude of the external force. It was found in Refs. [22,23] that this condition taken simultaneously with the conditions (15)-(17) of the arising of induced saddle states gives possibility to define quite accurately the regions of system control parameters where the chaotic state arise.

When applying Melikov's method, it should be remembered that this method gives in general case neither sufficient nor necessary conditions of the chaos onset. That is due to the following reasons. Melnikov's approach do not allow to determine whether or not the homoclinic structure associated with some saddle orbit is attractive, and hence, this approach can non be considered as sufficient. Besides, there may exist other saddle orbits in the phase space which may bring into existence other homoclinic structures. Because of it this method can not always give necessary condition for the chaos to arise. The application of Melnikov's technique should be always accompanied by additional detailed numerical experiments to check the accuracy of the analytical results. In this connection it is rather important to develop the alternative analytic approaches to determining the conditions for strange attractors to occur. Some of such promising approaches are discussed in the next two sections.

2.3.2. *Current Lyapunov exponents technique*

The current Lyapunov exponents technique is based on the investigation of the local properties of the motion on an attractor. The possibility of the constructive use of this technique to determine analytical conditions for the chaos onset was pointed out in the papers [24,25].

The current Lyapunov exponents are introduced in the following manner [24, 25]. Let an arbitrary dynamical system be specified by the ordinary differential equations

$$\dot{x} = F(x,t), \quad x \in R^n. \quad (2.21)$$

As in the usual procedure for determining Lyapunov exponents [50], let us write in the case of (2.21) a linearized system of equations which determines the evolution of an arbitrary vector **y** in the tangent space

$$\dot{y} = J(x,t)y, \quad (2.22)$$

where $J(x,t) = \partial F(x,t)/\partial x$ is the matrix of the linearized system.

Let us choose an arbitrary set of orthogonal vectors $\{\mathbf{y}_k\}$, $k=1, 2, \ldots, n$ in the tangent space. Then, the spectrum of the current Lyapunov exponents, which is denoted by $\mu_k(t)$, $k=1, 2, \ldots, n$, is introduced as the logarithmic derivative of the norms of these vectors

$$\mu_k(t) = \frac{d}{dt} \ln \|y_k\|. \quad (2.23)$$

The functions $\mu_k(t)$ are exponents of the local extension or contraction of the phase flow in the neighborhood of the trajectory $\mathbf{x}(t)$ in the direction of vectors $\mathbf{y}_k(t)$.

The use of current Lyapunov exponents enables one to characterize the properties of regular and chaotic attractors using the probability distributions of these quantities and their moments. A knowledge of $\mu_k(t)$ also enables the fractal dimension of attractors to be calculated immediately [49].

The relationship between $\mu_k(t)$ and the Lyapunov characteristic exponents λ_k, which are introduced in following manner [51]

$$\lambda_k = \lim_{T\to\infty} \frac{1}{T} \ln \frac{\|y_k(T)\|}{\|y_k(0)\|},$$

is of fundamental importance in the subsequent analysis.

It can be easily shown that, assuming the motion in an attractor to be ergodic, λ_k are found from $\mu_k(t)$ by averaging over time

$$\lambda_k = \lim_{T\to\infty} \frac{1}{T} \int_0^T \mu_k(t)dt, \qquad (2.24)$$

that is, λ_k are the first initial moments of the probability distributions for the quantities $\mu_k(t)$.

The relationship should be noted between current Lyapunov exponents and the effective (local) Lyapunov exponents $\lambda_k(\mathbf{x}(t), T)$ which, unlike $\mu_k(t)$, characterize the properties of extension or contraction of the phase flow after a certain finite time interval T. The relationship between $\mu_k(t)$ and $\lambda_k(\mathbf{x}(t), T)$ is given by the following expression

$$\mu_k(t) = \lim_{T\to 0} \lambda_k(\mathbf{x}(t), T).$$

In the general case non autonomous dynamical systems with one and a half degrees of freedom can be represented in the form

$$dx_1/dt = f_1(x_1, x_2, t), \quad dx_2/dt = f_2(x_1, x_2, t). \qquad (2.25)$$

Let us specify the expressions for the current Lyapunov exponents in the case of these systems. The equations, corresponding to system (2.25), for the amplitude ρ and the phase Φ of a vector in the tangent space have the form

$$d\rho/dt = \frac{\rho}{2}\left[f_{11} + f_{22} + (f_{11} - f_{22})\cos(2\Phi) + (f_{12} + f_{21})\sin(2\Phi)\right], \qquad (2.26a)$$

$$d\Phi/dt = \frac{1}{2}\left[f_{21} - f_{12} + (f_{21} + f_{12})\cos(2\Phi) + (f_{22} - f_{11})\sin(2\Phi)\right]. \qquad (2.26)$$

Here $f_{ij} = \partial f_i/\partial x_j\big|_{x_j = x_j^*(t)}$, where $x_j^*(t)$ is the jth coordinate of the trajectory of system (2.25). Then, when account is taken of the fact that $\|\mathbf{y}_1\| = \rho$ and that the angle between the vectors $\mathbf{y}_1$ and $\mathbf{y}_2$ in the tangent space is equal to $\pi/2$ by definition, from (2.23) and (2.26) we find the following expressions for the current Lyapunov exponents

$$\mu_{1,2} = \left[f_{11} + f_{22} \pm (f_{11} - f_{22}) \times \cos(2\Phi) \pm (f_{12} + f_{21})\sin(2\Phi)\right]/2 \qquad (2.27)$$

In particular, it follows directly from these relationships that the use of current Lyapunov exponents enables one to simplify appreciably the procedure for calculating the spectrum of the Lyapunov exponents $\lambda_{1,2}$ compared with the generally accepted technique [50]. This follows from the fact that, firstly, the quantities $\mu_{1,2}$, whose averages over time are identical to $\lambda_{1,2}$, are independent of the amplitude ρ and it is sufficient to integrate just one of the equations (2.26) for the phase Φ by determining the coefficients f_{ij} from the solution of the system of equations (2.25). Secondly, as follows from (2.27), no additional calculations (orthogonalization of vectors or additional integration) are required in order to find the second Lyapunov exponent.

The possibility of using current Lyapunov exponents for the analytic determination of the necessary conditions for the oscillations to become chaotic is attributable to the following. It follows from relationship (2.24) that the occurrence of chaotic oscillations ($\lambda_1 > 0$) is only possible when the maximum current Lyapunov exponent $\mu_1(t)$ is positive during finite intervals of time. Then, using expression (2.27) for μ_1 it turn out to be possible from the condition $\mu_1 > 0$ to determine the relationships between the controlling parameters of the problem. When these relationships are satisfied, chaotic oscillations can occur. Hence, the requirement of the existence of local instability of the trajectories of the phase flow is used as the necessary conditions for the oscillations to be chaotic. Of course, this conditions is not sufficient, since stretching of the phase flow may be compensated

by its contraction during traversal by the trajectories of other domains of phase space. It is found, however, that in the space of the controlling parameters, the limits of the existence of a local instability are often located fairly close to the boundaries of the domain of occurrence of global chaos ($\lambda_1>0$) and, hence, the use of this criterion enables one to predict fairly well the values of the parameters for which one observes the oscillations becoming chaotic.

Let us apply it to the system under consideration. We first write down the equation for the amplitude ρ and the phase Φ of a vector in the tangent space of the system (2.9)

$$\frac{d\rho}{d\tau} = (\rho - \alpha_0 - 2\alpha_1 a^2 + \\ + a^2\{\beta\sin[2(\Phi-\gamma]-\alpha_1\cos[2(\Phi-\gamma)]\})$$

$$\frac{d\Phi}{d\tau} = \Delta + 2\beta a^2 + a^2\{\beta\cos[2(\Phi-\gamma]+ \\ +\alpha_1 c\ \ 2\ \ \Phi-\gamma)]\}) \qquad (2.28)$$

The expression for the largest Lyapunov exponent can be written in the following form

$$\mu_1 = -\alpha_0 - \alpha_1 a^2\left\{-2+\sqrt{1+\beta^2/\alpha_1^2}\sin\left[2(\Phi-\gamma+\theta)\right]\right\}. \qquad (2.29)$$

where $\tan(2\theta)=-\alpha_1/\beta$.. From this expression we immediately obtain that positive values of $\mu_1(\tau)$ can only be attained when

$$\beta > \sqrt{3}\,\alpha_1 \qquad (2.30)$$

Hence, a necessary condition for the chaos onset is that the parameter of nonlinearity β should exceed a certain threshold determined by the value of the nonlinear dissipation. Note that this condition coincides with the condition (2.17) of the saddle state arising under the action of a harmonic perturbation. According to the expressions (2.28) (2.30), this condition does not depend upon the form and parameters of the external action. The inequality which is the inverse of (2.30) is the sufficient condition for the stability of the oscillator.

A second condition, which is necessary for the onset of chaos, is found from eq. (2.29) with respect to the amplitude $a(\tau)$. The function $\mu_1(\tau)$ can take positive values in finite time intervals only in the case when

$$\max\{a(\tau)\} > a_{th} \equiv \left[\frac{\alpha_0}{\left(\alpha_1^2+\beta^2\right)^{1/2}-2\alpha_1}\right]^{1/2} \qquad (2.31)$$

that is, the onset of chaotic oscillations is a threshold effect with respect to the amplitude forced oscillations. The condition (2.31) enables one to obtain an estimate for the smallest value of the amplitude of the spectral components of an external action, starting from which the development of stochastic instability is possible. In order to do this, we make use of the fact that the greatest amplitude of the excited oscillation of the harmonically forced oscillator does not exceed a value of $p_{th\alpha}$ and is identical to it when α_1. Let us assume that the amplitude of the second spectral component of the external action is relatively small which means that we may also adopt the above-mentioned value $p_{th\alpha}$ as an estimate of $\max\{a(\tau)\}$ in this case. Summing up what has been said, it is possible to write the following approximate condition for the onset of chaos

$$p_1 > p_{th} \equiv \alpha_0\left[\frac{\alpha_0}{\left(\alpha_1^2+\beta^2\right)^{1/2}-2\alpha_1}\right]^{1/2} \qquad (2.32)$$

When the nonlinear dissipation is small, then instead of (2.32) we have

$$p_1 > p_{th} \equiv \alpha_0\left[\alpha_0/\beta\right]^{1/2} \qquad (2.33)$$

This condition is identical to relationship (2.18a) apart from a factor which is close to unity. Thus, the condition for the chaos onset (2.33) is equivalent to the onset of saddle states during a harmonic action on the oscillator.

When the inequalities (2.30), (2.31) are simultaneously satisfied, then to obtain positive values of $\mu_1(\tau)$, it is that a certain "phase" condition should be satisfied, which according to eq. (2.29), is

$$\sin\left[2(\Phi-\gamma+\theta)\right] > 0,$$

which corresponds to the orientation of the vector in the tangent space in directions where its stretching occurs. The results of the paper [25] indicate that this condition takes place due to a parametric instability of the solution of the linearized equations (2.28), and it is typical mechanism of the chaos onset in passive single-degree-of-freedom system with external excitation.

2.3.3 Mapping.

Under some reasonable assumptions the distraction of quasiperiodic oscillations in weakly nonlinear oscillator can be reduced to the study of a discrete map [26,27]. To obtain the map for the equation (2.1), let us set the number of the spectral component of the external forcing equal to an infinity instead of the two ones in the following way

$$A_1 \cos\omega_1 t + A_2 \cos\omega_2 t \to \sum_{n=-\infty}^{n=\infty} A_n \cos(\omega_n t). \tag{2.34}$$

where $\omega_n = \omega_1 + n\varpi, \varpi = \omega_2 - \omega_1$. This new expression contains two incommensurable frequencies and, due to it, holds main properties of the previous one. When employ such substitution, we also use the well-known fact that the most significant influence on the behavior of the weakly nonlinear oscillator is exerted by the harmonic components of the external force with frequencies close to the natural frequency of the oscillator. One can expect that when $\varpi > \varepsilon\omega_0$, then the substitution will be almost equivalent. Assuming that all the amplitudes A_2 are equal to same value A_0 and using the following representation for the Dirac δ-function,

$$\sum_{n=-\infty}^{n=\infty} \cos(n\Omega\tau) = T\sum_{k=-\infty}^{k=\infty} \delta(\tau - kT),$$

where $T=2\pi/\Omega$, the system (2.10) is replaced by the following one[26]

$$\frac{dU}{d\tau} = -\left[\alpha_0 + \alpha_1\left(U^2+V^2\right)\right]U - \left[\Delta + \beta\left(U^2+V^2\right)\right]V$$
$$\frac{dV}{d\tau} = -\left[\alpha_0 + \alpha_1\left(U^2+V^2\right)\right]V +$$
$$+\left[\Delta + \beta\left(U^2+V^2\right)\right]U + A_0 T\sum_{k=-\infty}^{k=\infty}\delta(\tau - kT) \tag{2.35}$$

We come to the system of equations with an infinite sequence of the δ-pulses. Now let us use the fact that during the time intervals between the pulses, eqs (2.35) become autonomous. This allows one to write the solution of this system by connecting the solutions of the corresponding autonomous equations between neighboring δ-pulses. The result of that is the discrete map which for $\alpha_1 = 0$ takes the form

$$\bar{z} = z\exp\left[-\alpha_0 T + \left(i - \Delta T + E\mu\beta T|z|^2\right)\right] + A_0 T$$

Here $z = V(kT+0) + iU(kT+0)$ and $\bar{z} = V(kT+T+0) + iU(kT+T+0)$ are the complex variables representing the envelope of the oscillation at the time moments corresponding to two consequent, k-th and $k+1$-th, δ-pulses and $\mu = \left[1-\exp(2\alpha_0 T)\right]/(2\alpha_0 T)$.

Fixed and periodic points of the map (2.36) correspond to periodic
orbits in the phase space of the averaged equations (2.10) and, therefore, to two-dimensional tori of the initial equation. Thus, the problem of studying of a quasiperiodic motion of the weakly nonlinear oscillator is essentially simplified.

Each fixed point Z of the map on the complex phase plane z satisfies the equation $\bar{z}(Z) = Z$ which can be transformed to the following one

$$2\exp(\alpha_0 T)\left[\cosh(-\alpha_0 T) - \cos(-\Delta T + \mu\beta\Pi)\right]I = A_0 T^2 \tag{2.37}$$

where $I = |Z|^2$ is the intensity of the forced oscillations. Analyzing the stability of the fixed points, we obtain the following equation for the boundaries of the instability regions

$$\cos(-\Delta T + \mu\beta\Pi) +$$
$$+\mu\beta\Pi\sin(-\Delta T + \mu\beta\Pi) = \pm\cosh(\alpha_0 T) \tag{2.38}$$

Here sign (+) corresponds to the tangent (or saddle-node) bifurcation when one of the characteristic multipliers of the fixed point becomes equal to 1. This curve surrounds the regions of the existence of an induced saddle fixed point. Sign (-) in eq. (2.38) corresponds to the period-doubling bifurcation occurring when one of the characteristic multipliers becomes equal to -1. When the response curve of the oscillator (2.37) crosses over the latter region, the corresponding fixed point of the map undergoes the period-doubling bifurcation.

The boundaries of the chaos onset in a parameter plane are usually not far from that of period doubling. It allows to estimate the condition for chaos by using eq. (2.38). Let us suppose that $\exp(-\alpha_0 T) << 1$, then from eqs. (2.37),(2.38) one can obtain the following condition for the chaos onset

$$A_0^2\beta T^2 e^{-\alpha_0 T}\alpha^{-1} >> 1 \qquad (2.39)$$

The left-hand side of this condition achieves its maximal value when

$$\alpha_0 T = 2 \qquad (2.40)$$

It means that the most favorable conditions for the arising of the chaotic motion appear in the case when the relaxation time of the system has the same order as the period T. If the condition (2.40) is hold, then from eq. (2.39) we find the expression for the threshold value of the amplitude of the external force

$$A_{0thr} \cong 1.35\alpha_0^{3/2}\beta^{-1/2}$$

which coincides (with accuracy up to a numerical multiplier) with the same value found above (see eq. (2.33)).

3. Chaotic states of nonlinear oscillators with parametric excitation

The phenomena of parametric generation, amplification of oscillations and frequency conversion are distinguishing features of the dynamics of a variety of physical systems. For the non autonomous single-degree-of-freedom systems which are investigated in this paper, these phenomena can be adequately described within the framework of a universal mathematical model, like the motion equation of the following nonlinear oscillator:

$$\ddot{x} + +\omega_0^2\left[1 - \varepsilon M\cos\left(\omega_p t\right)\right]x =$$
$$= \varepsilon[-\left(\delta_0 + \delta_1 x^2\right)\dot{x} + \gamma x^3 + A\cos\left(\omega_s t\right)], \qquad (3.1)$$

subjected to combined parametric and external forcing. Here x is a generalized coordinate of the oscillator, ε is small parameter, $\delta_0 > 0$ and $\delta_1 > 0$ are the coefficients of linear and nonlinear damping, γ is the nonlinearity parameter, ω_0 is the natural frequency of the oscillator, M and A the amplitudes of parametric and external forcing with the incommensurate frequencies ω_p and ω_s. For example, in the case of optical and microwave parametric amplifiers, M and A are respectively proportional to the amplitude of a pumping oscillation and a signal wave to be amplified.

The unperturbed oscillator (3.1) possesses the same properties as that studied in the previous part of the paper (see (2.1)) with the same original saddle points and corresponding heteroclinic orbit (see fig.1). The condition of the homoclinic structure formation on the base of this orbit can be found by using the Melnikov method. The final result reads [7]

$$A\omega_s\,\mathrm{cosech}\left(\frac{\pi\omega_s}{\sqrt{2}\omega_0}\right) + \frac{M\omega_0^2\omega_p^2}{\sqrt{2\varepsilon\gamma}}$$
$$\mathrm{cosech}\left(\frac{\pi\omega_p}{\sqrt{2}\omega_0}\right) \geq \left|\frac{2\omega_0^3}{3\pi\sqrt{\varepsilon\gamma}}\left(\delta_0 + \frac{\delta_1\omega_0^2}{5\varepsilon\gamma}\right)\right| \qquad (3.2)$$

One can see from this equation that the chaotic oscillations can arise when there is only parametric excitation (A=0) or only external one (M=0). Under the combined excitation ($A\neq0$ and $M\neq0$), the threshold for chaos to arise is not changed essentially. It is easy to check that the formation of a homoclinic structure can take place only in the oscillator with a strong nonlinearity. In the weakly nonlinear limit ($\varepsilon\to0$) this criterion does not predict the chaos onset. However, the chaotic states are also typical for the parametrically forced oscillator (3.1) under weakly nonlinear excitation conditions. The mechanism of the chaos arising is determined by induced saddle states, and by the interaction of the parametric and external resonances. In this part of the paper we describe general conditions of the transition to chaos and study the properties of chaotic and regular states of the system (3.1). To carry out this plan we divide the problem into two parts. The first one is devoted to the investigation of the induced saddle states in the oscillator. We consider the case when the amplitude of the external forcing p is relatively small and the induced saddle states can arise mainly due to the parametric excitation. Thus, this problem is reduced to the study of the nonlinear parametric resonance (see Section 3.1). This case is of prime interest for many practical situations, for example, for microwave and optical parametric amplifiers where amplitude of the pumping wave ($\propto m$) is much more greater than that of signal wave ($\propto p$). The opposite case was considered by Yagasaki [28]. The second part of the problem deals with the formation of homoclinic structures on the base of the induced saddle states, and with phenomena pertaining to the chaotic states arising (see Section 3.2).

3.1 Nonlinear parametric resonance

Hereinafter we shall study the condition of the chaotic states arising in the weakly nonlinear os-

cillators, interesting in the case of the main parametric resonance when

$|\omega - \omega_0| = O(\varepsilon\omega_0)$, and $|\omega_s - \omega_0| = O(\varepsilon\omega_0)$ (3.3)

where $\omega \equiv \omega_p / 2$. Then, by using the transformation

$$x = U\cos\omega t + V\sin\omega t$$
$$y = -U\omega\sin\omega t + V\omega\cos\omega t, \qquad (3.4)$$

and neglecting by the terms $O(\varepsilon^2)$, we come to the following system of averaging equations for the slowly varying time functions $U(\tau), V(\tau)$:

$$\frac{dU}{d\tau} = -\left[\alpha_0 + \alpha_1\left(U^2+V^2\right)\right]U - \left[\Delta - m + \beta\left(U^2+V^2\right)\right]V - p\sin\Omega\tau$$
$$\frac{dV}{d\tau} = -\left[\alpha_0 + \alpha_1\left(U^2+V^2\right)\right]V + \left[\Delta + m + \beta\left(U^2+V^2\right)\right]U + p\cos\Omega\tau \qquad (3.5)$$

where dimensionless parameters are introduced: $\tau=\varepsilon\omega_p t/2$, $\alpha_0=\delta_0/\omega_p$, $\alpha_1=\delta_1/(4\omega_p)$, $m=M/4$, $p = 2A/\omega_p^2$, $\beta = 3\gamma/\left(2\omega_p^2\right) > 0$, $\Delta=(\omega_p-2\omega_0)/(\varepsilon\omega_p)$ and $\Omega=(\omega_p-2\omega_s)/(\varepsilon\omega_p)$.

Let us consider the conditions of the induced saddle states arising under the influence of the parametric modulation. Assuming that the dissipation and the external forcing are absent, we have instead of (3.5) the following Hamiltonian system:

$$\frac{dU}{d\tau} = -\left[\Delta - m + \beta\left(U^2+V^2\right)\right]V$$
$$\frac{dV}{d\tau} = \left[\Delta + m + \beta\left(U^2+V^2\right)\right]U \qquad (3.6)$$

with Hamiltonian energy given by

$$H(U,V) = -\frac{\beta}{4}\left(U^2+V^2\right)^2 - \frac{1}{2}\left[(\Delta - m)V^2 + (\Delta + m)U^2\right] \qquad (3.7)$$

As long as $m=0$, there is only a center-type singular point in the origin of the coordinate. For $m \neq 0$ one can find from (3.6) that the center is split into three or five singular points depending upon the relation between m and Δ. The two possible situations are illustrated by the phase portraits of the system (3.6) in fig.3. Note that these phase portraits constitute Poincare maps of the initial system for the case under consideration: $\delta_0 = \delta_1 = A = 0$, and small values of the amplitude of the forced oscillations. When $|\Delta|<m$, there are three singular points: a saddle point in the origin of the coordinates ($U=0$, $V=0$) and two centers with coordinates $(U,V)=(0, \pm\sqrt{(m-\Delta)/\beta})$ which

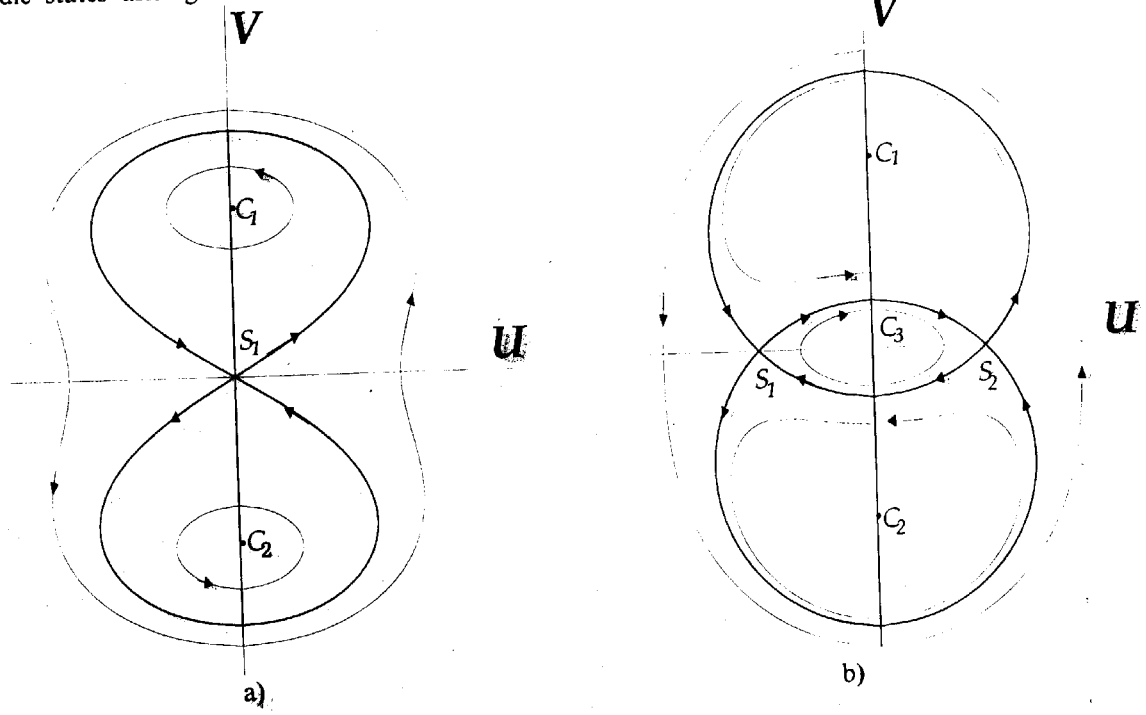

Fig.3. *Phase portraits of the Hamiltonian system (3.6) for: (a) $|\Delta|<m$ and (b) $|\Delta|>m$.*

are denoted in fig.3a as C_1, C_2. In the second case, when $|\Delta|>m$, there are three centers C_1, C_2, C_3 and two saddle points with coordinates $U=\pm\sqrt{(-m-\Delta)/\beta}, V=0$ in the phase space as shown in fig.3b. Because of these saddle points, the system possesses induced homoclinic or heteroclinic orbits (separatrix) indicated in fig. 3. Owing to the induced centers, the system acquires a multistability property when $\alpha_0 \neq 0$ (see below).

Let us consider in more detail the structure of the separatrix loops for the two cases. For $|\Delta|<m$, there is a double symmetric saddle loop. The solution of the motion equation $U\equiv U_l(\tau)$ and $V_l\equiv V_l(\tau)$ on this separatrix was found in Ref.[29] and can be written in the form:

$$U_l^2(\tau)=\frac{4b_1^2b_2\left(1-\cosh\left[a_1(\tau-\tau_0)\right]\right)}{\left((b_1-b_2)\cosh\left[a_1(\tau-\tau_0)\right]-b_1-b_2\right)^2}, \tag{3.8}$$

$$V_l^2(\tau)=\frac{4b_1b_2^2\left(1+\cosh\left[a_1(\tau-\tau_0)\right]\right)}{\left((b_1-b_2)\cosh\left[a_1(\tau-\tau_0)\right]-b_1-b_2\right)^2},$$

where $b_{1,2}=(\pm m-\Delta)/\beta$, $a_1=2\beta\sqrt{-b_1b_2}$, τ_0 is an initial moment of the "slow" time

In the second case shown in fig 3b, because of the two saddle points, double heteroclinic loops arise: the small and large ones. After intensive calculations one can find the following equation of these loops:

$$U_l(\tau)=-\frac{\sqrt{b_2}(b_1+b_2)\sinh\left[a_2(\tau-\tau_0)\right]}{(b_1+b_2)\cosh\left[a_2(\tau-\tau_0)\right]-q_\pm(b_1-b_2)}, \tag{3.9}$$

$$V_l(\tau)=-\frac{\sqrt{2(b_1-b_2)}b_2q_\pm}{(b_1+b_2)\cosh\left[a_2(\tau-\tau_0)\right]-q_\pm(b_1-b_2)},$$

where $a_2=\beta\sqrt{2b_2(b_1-b_2)}$, $q_\pm=\pm\sqrt{(b_1+b_2)/(b_1-b_2)}$, q_+ and q_- correspond to the large and small loops of the separatrix, accordingly.

The regions in the parameter space where the saddle states exist are reduced under the influence of dissipation. However, for any value of the linear ($\alpha_0<\infty$) and nonlinear ($\alpha_1<\infty$) dissipation these regions have finite dimensions. Let us show it by introducing into the consideration the corresponding dissipative terms into the system (3.6), thus we have

$$\frac{dU}{d\tau}=-\left[\alpha_0+\alpha_1\left(U^2+V^2\right)\right]U-$$
$$-\left[\Delta-m+\beta\left(U^2+V^2\right)\right]V, \tag{3.10}$$

$$\frac{dV}{d\tau}=-\left[\alpha_0+\alpha_1\left(U^2+V^2\right)\right]V$$
$$+\left[\Delta+m+\beta\left(U^2+V^2\right)\right]U.$$

This system yields the following equation for the equilibrium states.

$$\Delta=-\beta W^2\pm\sqrt{m^2-\left(\alpha_0+\alpha_1W^2\right)^2}, \tag{3.11}$$

where $W^2=U^2+V^2$ and W is the amplitude of oscillation. Note that $W=0$ is also an equilibrium state. The amplitudes of stationary states versus Δ (the response curve of the oscillator) are shown in fig.4. The saddle states are marked by dashed curve. It is easy to check that the saddle states with $W=0$ exist in the following parameter region:

$$\alpha_0<m. \tag{3.12}$$

$$\Delta<-\sqrt{m^2-\alpha_0^2}. \tag{3.13}$$

whereas such states with $W\neq0$ exist when

$$\beta\alpha_0-m\sqrt{\alpha_1^2+\beta^2}<\Delta<-\sqrt{m^2-\alpha_0^2}, \tag{3.14}$$

provided that the amplitude of modulation m satisfy simultaneously the condition (3.12) and the following one

$$\beta\alpha_0-m\sqrt{\alpha_1^2+\beta^2}<-\alpha_1\sqrt{m^2-\alpha_0^2}. \tag{3.15}$$

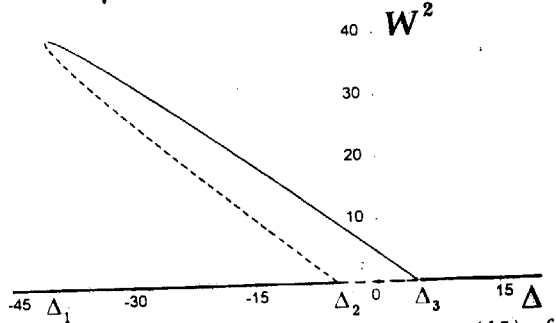

Fig.4. *Response curve of the system (15) for $\alpha_0=1$, $\alpha_1=0.1$, $\beta=1$, $m=5$. Solid curves correspond to stable states and dashed ones - saddle states. The boundaries of the regions with different types of the system behavior are*

$$\Delta_1=\left(\beta\alpha_0-m\sqrt{\alpha_1^2+\beta^2}\right)\Big/\alpha_1,$$

$$\Delta_{2,3}=\pm\sqrt{m^2-\alpha_0^2}.$$

The above given conditions (3.12)-(3.15) determine the regions in the parameter space where Melnikov's method can be applied to the system (3.5). These conditions should be considered as additional ones to Melnikov's criterion of the chaos arising that will be obtained in the next sections. They determine the threshold of the chaos arising with respect to the amplitude of the parametric force and the resonant condition for the chaos to exist.

3.2. Chaotic states of the oscillator with induced heteroclinic orbits

In this section we illustrate the mechanism of the transition to chaos for the oscillator with the heteroclinic orbits associated with the pair of saddle points as shown in fig.3b. The second case was considered in Ref. [29]. We start from the application of Melnikov's method to the averaged equations (3.5) to find necessary conditions for the chaos onset. Performing the corresponding calculation in the way similar to that described in the Section 2.3, we come to the following condition of the manifolds' intersections:

$$p \geq \left| \frac{2\sqrt{m/\beta}\,\sinh(\pi\sigma_2)}{\pi\Omega \exp\left(\pm\sigma_2 \arccos\left(m\sqrt{-\frac{m}{\Delta}}\right)\right)} \times \right.$$

$$\times \left\{ \alpha_0 \left[r_2 \mp \Delta \arccos\left(\mp\sqrt{-\frac{m}{\Delta}}\right)\right] - \right.$$

$$\left. \left. - \frac{\alpha_1}{\beta}\left[3r_2\Delta \pm \left(2m\Delta - \Delta^2\right)\arccos\left(\mp\sqrt{-\frac{m}{\Delta}}\right)\right]\right\}\right| \qquad (3.16)$$

Here $r_2 = \sqrt{-m(\Delta+m)}$, $\sigma_2 = \Omega/(2r_2)$.

A typical example of the bifurcation diagram in the parameter plane (p,Ω) obtained numerically along with Melnikov's criterion (curve 1) are given in fig.5. The best way to explain all possible behavior of the system is to start from the Hamiltonian case, i.e., fig.3b, and then put $\alpha_0 \neq 0$. We obtain three stable foci instead of three centers, and all trajectories will eventually come to one of them, depending on initial conditions. The attractors which arise in the vicinity of

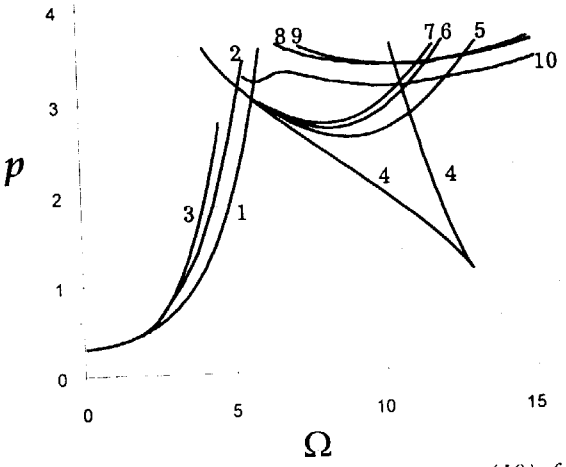

Fig.5. *Bifurcation diagram of the system (10) for and α_0=1, α_1=0, β=1, Δ=-6, m=5. Curves 1-3 correspond to the attractors formed on the base of the small heteroclinic loop: (1) boundary of homoclinic structure existence according to Melnikov's criterion, (2) - symmetry breaking, (3) - first period doubling bifurcation. Curves 4-6 correspond to the attractors due to the saddle orbit induced by the external force: (4) - tangent bifurcation, (5) and (6) - first and second period doubling bifurcations, (7) - attractors crises. Curves 8, 9 correspond to the attractors formed on the base of the large heteroclinic loop, and represent boundaries of homoclinic structure existence found numerically and with Melnikov's criterion correspondingly. Curve (10) denotes the boundary of the strange attractors arising due to the intersection of stable manifold of the small loop and unstable manifold of the large loop.*

the centers C_1,C_2,C_3 we shall mark as A_1,A_2,A_3 accordingly. That is, the system is three-stable initially. Provided that the amplitude p is small enough, the foci turn to stable periodic orbits, and the three of them will exist simultaneously in the phase space. The attractor A_3 undergoes the symmetry breaking crises on curve 2, and to the left of this curve four attractors (A_1,A_2,A_3,A_3') coexist in the phase space. At curve 3 both attractors A_3,A_3' undergo the first period doubling bifurcation, and then a pair of strange attractors appears through the period doubling cascade. In fig. 6a the situation is given, when these two attractors merge and a unified strange attractor arises. It turns out that the strange attractors here are very sensitive to the variation of parameters and exist only in very narrow band adjacent to curve 3. Obviously, their basins of attraction are small and the majority of

initial conditions lead to two stable attractors co-existing with them.

In this region of the parameter plane the strange attractors arise due to the manifolds' intersections of the small loop, and other roads to chaos were not observed. In this case Melnikov's criterion works well and good predictions can be developed on its basis.

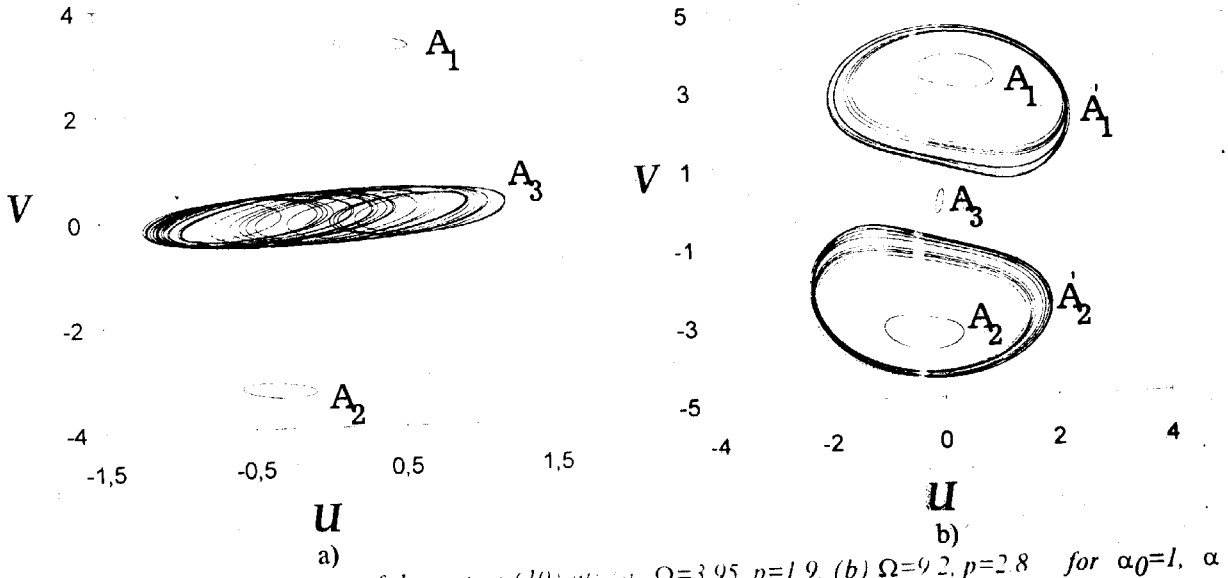

Fig.6. *All coexisting attractors of the system (10) at (a) Ω=3.95, p=1.9, (b) Ω=9.2, p=2.8 for α_0=1, α_1=0, β=1, Δ=-6, m=5.*

Clearly our way of the Melnikov's technique application does not allow to predict the appearance of these strange attractors. However, it can be done by considering the parametric force as a perturbation, rather then the external force.(see, i.e., Ref. [28]).

The intersections of the manifolds of the large loop associated with the parametrically induced saddles $S_{1,2}$ (see fig. 2b) took place at relatively large values of the external amplitude indicated by curve 8 in fig. 5. This curve practically coincides with that found from Melnikov's criterion (curve 9). One can conclude that this criterion works here well again. The chaotic oscillations exist in a narrow layer adjacent to these lines, and they arise through the period doubling cascade. We have not detected here any significant influence of the saddle orbits arising after each doubling bifurcation on the system dynamics. Instead, another layer-like chaotic region has been found next to curve 10 with a peculiar kind of the homoclinic structure formation. In this region the chaos onset is due to the intersection of the manifolds of different loops - large and small ones, not some of them. This situation is illustrated in fig.7, where the crossings of the unstable manifold of the large loop with the stable manifold of the small loop take place. To our knowledge, such mechanism of the transition to chaos has never been observed. It is interesting to find other system exhibiting this road to case, as well as to develop an analytical tool to detect the presence of such homoclinic structure.

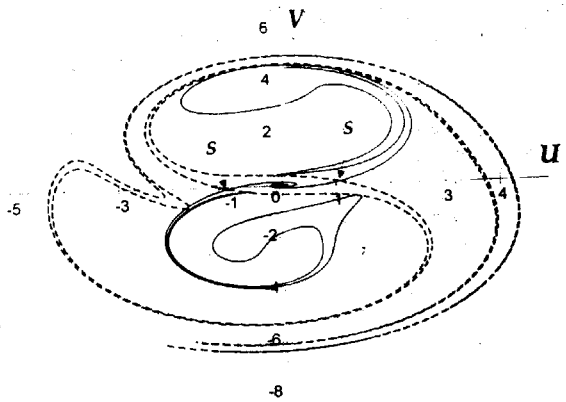

Fig.7. *Intersections of stable (dashed curve) manifold of the small loop and unstable (solid curve) manifold of the large loop in the Poincare section for p=3.2, Ω=12, α_0=1, α_1=0, β=1, Δ=-6, m=5.*

3.3. Chaos and stability of practical devices

In this section, we have considered the conditions of the chaotic states arising in the weakly nonlinear Duffing-type oscillators subjected to the combined parametric and external forcing. It was shown that homoclinic or heteroclinic orbits induced by one of the external harmonic component play crucial role in the oscillator dynamics. Because of these orbits the formation of a homoclinic structure tooks place here in the weakly nonlinear limit under the action of the another incommensurate frequency, and the chaos onset is due to the distraction of two-dimensional torus. The generality of these results does not depend on the perturbations, being considered, and they most probably hold for a variety of single-degree-of-freedom systems with quasiperiodic forcing.

We have also detailed some of phenomena which accompany the chaos onset. Multistability of the oscillator conditioned by the formation of several attracting sets in the phase space is one of such phenomenon. This study along with the foregoing ones [22, 30] suggests that the multistability is a typical feature of the quasiperiodically forced weakly nonlinear oscillators. It has been shown in this paper that the splitting of a center-type singular point into several stable and unstable orbits under the action of the periodic force is primarily responsible for the multistability property of the oscillator, at least for relatively small values of the force amplitude.

This study along with the previous results indicates that there are three typical roads of strange attractors arising depending upon the mechanism of the homoclinic structure formation. Let us cite them as they are seen in term of the averaged equations. The first road is through the intersection of the stable and unstable manifolds of some parametrically or externally induced homoclinic or heteroclinic loop. The second road described in ref. [7] is through the manifolds' intersections of an additional saddle orbit arising after one of the period doubling bifurcation. The third one is through the intersection of the stable and unstable manifolds associated with different loops (see fig. 7)

An important motivation for this work was results of experimental investigations of microwave parametric amplifiers which indicated that the amplifiers being stable under the action of only pumping oscillation or signal wave lose their stability when this oscillation and the signal wave are applied simultaneously [31]. The results of this paper give an explanation of such phenomenon and provide mathematical tools for its study and prediction. It is also obviously that our results are applicable, within certain limits, to other types of similar devices, say, Josephson-junction parametric amplifiers, optical amplifiers, etc. It is worth noting that the factors which are responsible for the chaos onset in the weakly nonlinear limit and, hence, for the low stability threshold of the parametric amplifiers are precisely the same as that providing low noise amplification from the point of view of the conventional theory of parametric devices. Indeed, according to the classical results of this theory, parametric amplifiers posses a low noise output level because they consist of a reactive circuit (anharmonic oscillator) and they utilize an ac power supply (pumping oscillation). In the mathematical model used the reactive type of nonlinearity is described by the term with parameter γ (see (3.1)). Proceeding from the obtained results, it is clear that exactly the combination of this type of nonlinearity and the parametric excitation leads to the possibility of the chaos onset in the weakly nonlinear limit when the external signal is applied. This is the main reason why the parametric amplifiers are extremely susceptible to the chaotic instabilities. These findings work also for Josephson-junction parametric amplifiers, SQUIDs and other types of similar devices.

4. Interaction of low- and high-frequency oscillations

Up to now we have considered the destruction of the quasiperiodic oscillations under the resonant excitation conditions which take place for each of the spectral components of the external forcing (see (2.7), (3.3)). However, the transition to chaos in weakly nonlinear oscillators is observed when the resonant condition is fulfilled only for one of the spectral components. An additional perturbation may act in a nonresonant manner, and it can be a low-frequency external force or a low-frequency modulation of an oscillator's parameters. There are several evidences that the chaotic states arise in weakly nonlinear systems under such excitation conditions. For example, it was shown in ref. [32], that the synchronized Gunn-diode oscillators can go into chaotic regimes of oscillations under the influence of a low-frequency hindrance in a supply circuit. The low-frequency modulation of the parameters of an electron beam exerts strong influence on the operation regimes of BWO tubes and free-electron lasers [33]. It was demonstrated recently [34, 35], that the interaction of low- and high frequency oscillations can limit the attempts of obtaining a large range of frequency deviation in varactor circuits.

In this part of the paper the problem stated is considered on a specific example, namely, dynamics of quantum magnetometers (SQUIDs) [36].

Such devices are widely used to record and measure extremely small magnetic fields or other quantities associated with them. The key element of magnetometers is a superconducting quantum interferometer which is a superconducting ring closed by a Josephson junction (see fig. 8). The interferometer is inductively coupled to a resonant oscillatory circuit which is excited (pumped) by an external harmonic oscillation. The change in the impedance of the interferometer introduced into the circuit leads to a change in the amplitude of the alternating potential in the circuit which enable one to record variations in external magnetic fields.

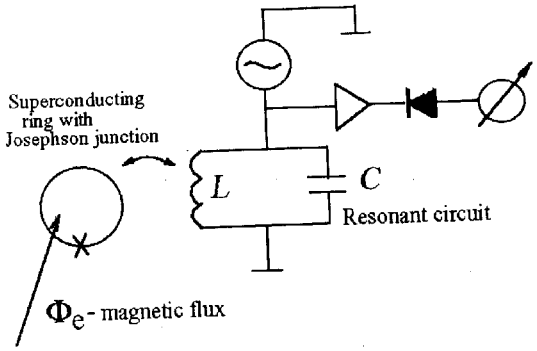

Fig.8. *Schematic diagram of the one-contact SQUID.*

A great deal of work has been done to study chaotic instabilities of SQUIDs (see, i.e.,[37-39]). Most of the studies are based on the assumption that a "chaotization" of the $\phi(t)$ phase of a SQUID wavefunction is supposed to be the main cause of the chaos onset. In this case, the time variation of the phase can be obtained as a solution of the generalized pendulum equation

$$\frac{1}{\omega_0^2}\frac{d^2\hat{\phi}}{dt^2}+\alpha\frac{d\hat{\phi}}{dt}+\hat{\phi}+l\sin\hat{\phi}=\varphi_e+A\cos\omega t \qquad (4.1)$$

where $\hat{\phi}$ is the normalized phase, ω_0 is the intrinsic interferometer frequency, α is the dissipation coefficient, l is the dimensionless inductance, ϕ_e is the normalized external magnetic flux, and A and ω are the external pumping amplitude and frequency, respectively.

The first term in eg. (4.1) describes the bias current passing through the Josephson junction, and it is defined by a junction capacity. The presence of the bias current is required for the chaotic oscillation excitation, as it is seen from the above equation. However, in most practical SQUIDs, the junction capacity effect on their dynamics can be reduced by shunting that allows for the intrinsic interferometer frequency to become significantly higher than the pumping frequency. Then, a simplified model follows from eg.4.1

$$\alpha\frac{d\hat{\phi}}{dt}+\hat{\phi}+l\sin\hat{\phi}=\varphi_e+A\cos\omega t \qquad (4.2)$$

This equation has no chaotic solutions, and hence, in this case, the chaotic solutions will not be typical for the model (4.1). Then the question arises: can we observe the chaotic instabilities in such magnetometers?. The investigations described below give an affirmative answer to this question. We shall show that exactly the interaction of the high- and low-frequency oscillations gives rise to the chaos onset, and that this phenomenon causes a limitation on the sensitivity of SQUIDs.

4.1. Mathematical model of weakly nonlinear SQUIDs

Let us write equations which describe the interaction of the interferometer with the SQUID circuit. For the SQUID shown in fig 8, these equations are as following [40]

$$\frac{d^2\phi_c}{dt^2}+\frac{\omega_c}{Q}\frac{d\phi_c}{dt}+\omega_c^2\phi_c=2b\omega_c^2\cos\omega t+k^2\omega_c^2 I_J \qquad (4.3)$$

$$\alpha\frac{d\hat{\phi}}{dt}+\hat{\phi}+l\sin\hat{\phi}=\varphi_e+\phi_c\equiv I_J \qquad (4.4)$$

where ϕ_c is the normalized voltage across the circuits, ω_c and Q the natural frequency and Q-factor of the circuit, k is the coefficient of coupling between the circuit and the superconducting ring, b is the normalized pumping amplitude, I_J is the normalized Josephson junction current.

In order to simplify this system, we take into account that for practical devices the following conditions have place

$$Q>>1,\quad k^2<<1,\quad |\omega-\omega_c|/\omega<<1$$

Due to these conditions the solution of the system (4.3), (4.4) can be seeking in the form of a quasiharmonic oscillation

$$\phi_c(t)=a(t)\cos[\omega t-\gamma(t)]$$

where amplitude $a(t)$ and phase $\gamma(t)$ are slow varying functions of time which can be found from the following system of averaged equations

$$\frac{da}{d\tau} = -a - b\sin\gamma$$
$$a\frac{d\gamma}{d\tau} = -\Delta a + RJ_1(a)\cos(\phi_e) - b\cos(\gamma) \quad (4.5)$$

Here $\Delta = (\omega - \omega_0)2Q/\omega$ is the normalized frequencies shift, $R = 2k^2Ql$ is the parameter of nonlinearity, $\tau = t\omega/2Q$ is the "slow", time, and $J_1(a)$ is the first-order Bessel function. For a more illustrative representation of the subsequent results, we restrict ourselves to an adiabatic SQUID model that corresponds to $\alpha = 0$ in eg. (4.4). However, it should be emphasized that taking the finite value of α into account does not practically affect the structure of egs. 4.5 (see ref. [40]), and the following results should also be true for this case.

By holding the coefficients in egs (4.5) constant in time, only the constant values of $a=A$ and $\gamma=\Gamma$ satisfying the equations

$$A^2 + \left[RJ_1(A)\cos(\phi_e) - \Delta A\right]^2 = b^2$$
$$\tan\Gamma = A/[\Delta A - RJ_1(A)\cos\phi_e] \quad (4.6)$$

can be considered as its solution for $\tau \to \infty$.

The situation changes qualitatively if the external magnetic flux ϕ_e,, which is an additive sum of the measured signal and biased flux, is considered to be a function of time. Consider the case when ϕ_e, is given by

$$\phi_e = \phi_0 + \phi_1\cos(\Omega\tau) \quad (4.7)$$

where ϕ_0 is the constant flux component, ϕ_1 is the alternating component amplitude, and Ω is the dimensionless frequency. The frequency of variation of the magnetic flux $\omega_m = \Omega\omega/2Q$ is considerably less than ω, i.e., the effect of the low-frequency magnetic flux variations is considered in our analysis. The interaction of this low-frequency oscillation with the pumping oscillation leads to the transition of chaos in the weakly nonlinear limit. Because of the pumping, the induced saddle states arise in the phase space of the system (4.5), which are of prime cause of the homoclinic structures formation under the low-frequency modulation. An analysis of solutions of eg. (4.6) and their stability shows that the induced saddle states arise under the following conditions

$$R > 4,\ b > b_{cr} = 5/\sqrt{R},\ |\Delta| < \Delta_{cr} = R/2 - \sqrt{3} \quad (4.8)$$

In the next section these conditions of the chaos onset will be supplemented with that obtained in the framework of the current Lyapunov technique. It is interesting to note that approximately the same conditions as given above were proposed in refs. [40] to use for the increasing of the SQUID sensitivity, however, the expected high-sensitivity level has not been achiever. The chaotic instability is probably one of the possible causes.

4.2. Conditions for the chaos onset

The chaotic instability of SQUIDs can take place if the values of the parameters satisfy the conditions (4.8), then for periodic variations in ϕ_e with the frequency $\Omega \geq 1$, one can observe the excitation of chaotic oscillations at a relatively small modulation amplitude ϕ_1. To obtain additional relations between parameters that can cause the chaotic instability, let us use the current Lyapunov exponents (see Appendix) for the system (4.5). With this purpose we linearize egs.(4.5) in the vicinity of arbitrary solution $a^* = a(\tau), \gamma^* = \gamma(\tau)$ The equations for the amplitude ρ and phase Φ of the perturbation vector can then be written in the form

$$\frac{d\rho}{dt} = \rho\left\{-1 + \frac{R\cos\phi_e}{2}\left[J_0(a^*) - 2\frac{J_1(a^*)}{a^*}\right]\times\right.$$
$$\left.\times\sin 2(\Phi - \gamma^*)\right\}$$
$$\frac{d\Phi}{dt} = -\Delta + \frac{R\cos\phi_e}{2}\left\{J_0(a^*) + \left[J_0(a^*) - 2\frac{J_1(a^*)}{a^*}\right]\times\right.$$
$$\left.\times\cos 2(\Phi - \gamma^*)\right\} \quad (4.9)$$

From these equations, the expression for the maximum current Lyapunov exponent follows

$$\mu_1(\tau) = -1 + \frac{R}{2}\cos\left(\phi_0 + \phi_1\cos(\Omega\tau)\right)\times$$
$$\times\left[J_0(a^*) - 2\frac{J_1(a^*)}{a^*}\right]\sin\chi\,. \quad (4.10)$$

where the phase $\chi(\tau) = 2(\Phi - \gamma^*)$ is defined from the equation

$$\frac{d\chi}{d\tau} = R\cos(\phi_0 + \phi_1\cos(\Omega\tau)) \times \times\left[J_0(a^*) - 2\frac{J_1(a^*)}{a^*}\right](1+\cos\chi) + \frac{2b}{a^*}\cos\gamma \; * \tag{4.11}$$

According to eg.(4.10), two conditions have to be satisfied, i.e., (i) the χ phase should predominantly take on the values corresponding to a direction of extension, $\sin\chi > 0$; (ii) the prefactor of $\sin\chi$ in eg.(4.10) should exceed unity at the finite-trajectory parts. With allowance made for the maximum value of the function $[J_0(a) - J_1(a)/a]_{\max} \cong 0.5$, it follows that the second condition is satisfied only when the relation

$$\left|\frac{R}{4}\cos(\phi_0 + \phi_1\cos(\Omega\tau))\right| > 1 \tag{4.12}$$

is met for finite intervals of variation in τ. Thus, the occurrence of chaotic oscillations is possible only when

$$R \equiv 2Q^2kl \geq 4. \tag{4.13}$$

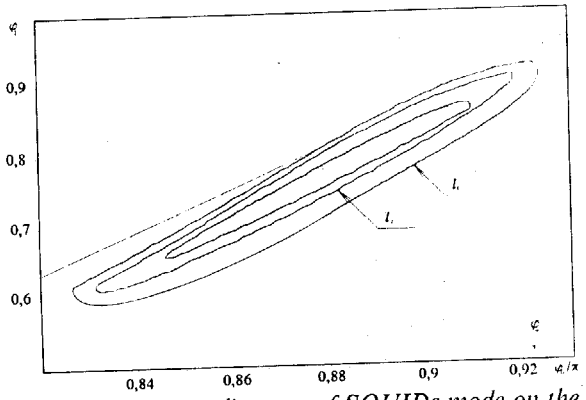

Fig.9 *Bifurcations diagram of SQUIDs mode on the parameter plane for R=10, b=3, Ω=1, Δ=-1. The lines of the period-doubling bifurcations are l_1 and l_2. The dashed line defines the boundary of the region where in agreement with eg. (10) local extension of the phase flow can occur.*

By assuming some values from eg.(4.12) for $R>4$, it is easy to find limits of those regions for ϕ_0 and ϕ_1 wherein a transition to chaos can be observed. In fig.9, one such boundary defined from eg.(4.12) at $R=10$ is shown by a dashed line on the plane of ϕ_0, ϕ_1 parameters, i.e.

$$\phi_1 = \phi_0 + \arccos(4/R) - \pi \tag{4.14}$$

Below this line, condition (4.12) is satisfied. At the same plane, a region of the chaotic system behavior defined by means of the numerical analysis is shown by dots. This region adjoins the analytic curve, confirming the assumption that the phase-flow extension (according to eg.(4.12)) immediately causes the chaotization of oscillations. The chaotic oscillations, however, cannot exist over a whole region of parameters defined by eg.(4.12), since the above condition for the χ-phase stabilization in the extension direction should be fulfilled simultaneously with eg.(4.12).

The investigations of the SQUID stability permit the following conclusions to be made [36].

1. The generation of chaotic oscillations in SQUIDs is possible in a quasilinear regime of operation as well, the interferometer excitation mode being nonhysteretic and interferometer processes approaching adiabatic and equilibrium ones. In this case, the interferometer can be regarded to occur nonlinear element in a SQUID circuit.

2. The chaotic instability arises due to the interaction of the low-frequency variations of the external magnetic flux and the pumping oscillation. It is clear that not only the variations in the magnetic flux but pumping amplitude and frequency variations as well can initiate the transition to chaos.

3. The results obtained allow the assumption to be made that limited SQUID sensitivity observed in some experiments may be explained by noise oscillations generated due to the chaotic instability.

5. Chaotic dynamics of two-mode systems

Multimode nature of the variety of physical systems creates a number of additional ways for the transition to chaos in the weakly nonlinear limit. Now it is clear that even two interacting weakly nonlinear modes can exhibit the chaotic behavior. It can be two active modes as well as one active and one passive modes [41]. We call a single mode passive when it is in a state before a Hopf bifurcation in contrast to the active modes which have undergone this bifurcation. The autonomous systems with the interaction of a passive mode with the active one may be considered as the simplest physical systems when the chaotic states can arise. According to this, for example, the transi-

tion to turbulent flows in bounded volumes can be as following. As the result of an increase of a non-equlibrium parameter's value of the system (e.g., the Reynolds or Rayleigh number), a periodic motion has arisen due to the Hopf bifurcation, and a single-mode oscillation has been established. Then, because of the interaction of this active mode with one of the infinite number of passive modes, the turbulent flow is formed. This scenario is realized under weakly nonlinear excitation conditions, and it is worth consideration as a typical way to turbulence.

Two passive weakly nonlinear interacting modes with a periodic forcing is the simplest non autonomous multimode system with the chaotic behavior. The mathematical model of this system, typical for many applications, consists of two coupled weakly nonlinear Duffing-type oscillators with an external harmonic force. To simplify its study, the method of averaging can be used which results in the following system of equations [42]

$$\begin{aligned}
\frac{da}{d\tau} &= -\alpha_0 a - \alpha_1 a^3 - k_1 b\sin(\psi-\varphi) - P\sin\psi \\
\frac{d\psi}{d\tau} &= -\Delta - \beta a^2 - k_1\frac{b}{a}\cos(\psi-\varphi) - \frac{P}{a}\cos\psi \\
\frac{db}{d\tau} &= -\delta b - k_2 a\sin(\psi-\varphi) \\
\frac{d\varphi}{d\tau} &= -\Delta + \mu - k_2\frac{a}{b}\cos(\psi-\varphi)
\end{aligned} \tag{5.1}$$

with respect to the amplitudes a,b and phase ψ,φ of the interacting modes. These equations are given for the case when only one of the modes is linear and the second mode is nonlinear. This situation was considered in Ref. [42], and a good correspondence between theoretical and experimental results were observed. In some aspects the mechanism of the transition to chaos here is similar to that described for the quasiperiodically forced oscillator in Section 2. In the both cases the prime reason for chaos is the induced saddle states that arise due to the external forcing. Then, under the additional perturbation, which is coupled linear mode in the above given system (5.1), a homoclinic structure is formed on the base of one of the induced saddle states. The application of the current Lyapunov technique to the system (5.1) leads to the following necessary conditions for the chaos to arise

$$\beta > \sqrt{3}\alpha_1 \tag{5.2a}$$

$$P^2 > \frac{8\alpha_0^3}{3\sqrt{3}\beta} \tag{5.2b}$$

which are similar to that given by egs (2.17c), (2.18a).

When studying the dynamics of multimode weakly nonlinear systems, two types of the modes interaction are introduced: resonant and nonresonant one. Usually, the resonant interaction is considered as that giving rise to chaos. However, it was shown in Ref. [43,44], that nonresonant interaction can play an important role in the formation of chaotic states. The two-mode interaction in the presence of an external harmonic forcing was investigated by using the following system of the averaged equations

$$\begin{aligned}
\frac{da}{d\tau} &= (\alpha_a - \gamma_a a^2 - \mu_a b^2)a + R\sin\varphi \\
a\frac{d\varphi}{d\tau} &= (-\Delta + \beta a^2 + \kappa b^2)a + R\cos\varphi \\
\frac{db}{d\tau} &= (\alpha_b - \gamma_b b^2 - \mu_b a^2)b
\end{aligned}$$

Here a and b are the dimensionless amplitudes of the modes which are interacting nonresonantly with each other, φ is the phase of external force.

It was shown in Refs. [44] that nonresonant interaction of two active modes as well as active and passive ones leads to the chaos onset when the parameters of the modes coupling go over some critical values. The mechanism of the transition to chaos is related with the occurrence of an induced homoclinic loop in the phase space of this system.

In this part of the paper we shall study in more details the dynamics of the above mentioned autonomous system with two interacting modes: passive and active ones. This problem is considered with respect to the investigation of the complicated behavior of variable stars. At first, we outline the derivation of the equations for interacting modes for this problem.

5.1. Mathematical model of stellar pulsations

According to present-day status of research, a number of laws of the behavior of variable stars is explained by arising of the stellar radial oscillations which is caused by exciting of one or more hydrodynamical eigenmodes. The development of this conception made it feasible to reduce such the stellar dynamics research to the analysis of solutions of the ordinary differential equations for the

amplitudes and phases excited modes. By using such models, the main peculiarities of the regular stellar pulsations occurrence have been studied in Refs. [45, 46], and later it was shown that such models can be generalized to study the irregular stellar pulsation [47].

Let us consider the standard hydrodynamic method of the stellar dynamics. The hydrodynamic equations on the assumption of spherical symmetry of a star take the form :

$$\frac{^2R}{t^2} = -4\pi R^2 \frac{\partial P}{\partial m} - \frac{Gm}{R^2} \equiv -g(R,s)$$

$$\frac{s}{t} = -\frac{1}{T}\frac{\partial L}{\partial m} \equiv h(R,s) \qquad (5.3)$$

$$\frac{\partial R^3}{\partial m} = \frac{3}{4\pi\rho}$$

with corresponding boundary conditions at inner and outer boundaries of the pulsating envelope [45, 46] These equations relate the Lagrange radius R, the pressure P, the density ρ, the specific entropy s of a spherical shell. They are the third order equations with respect to time and the fourth order ones to the mass m. Here

$$L \equiv (4\pi R^2)^2 \frac{a\,c}{3\kappa(\rho,T)}\frac{\partial T^4}{\partial m},$$

where κ is Rosseland mean opacity. The equation of state should be specified in the form: $s=s(\rho,T)$, $P=P(\rho,T)$.

The time independent solution (R_0, s_0) of the above set of equations can be obtained by setting $\frac{d}{dt}=0$. Further, it is assumed that the system (5.3) performs only small vibrations in the neighborhood of (R_0, s_0) and only variations $\delta R \equiv R-R_0$, $\delta s \equiv s-s_0$ have to be considered. Then by using the expansion of the solution in term of the eigenfunctions of the corresponding linear operator, one can reduce this problem to the study of the dynamics of interacting modes. In order to describe stellar pulsations, it is reasonable to take into consideration only the active eigenmodes (i.e., with positive real part of the complex eigenvalues) and the passive ones which interact in resonance manner.

We consider the two-mode interaction when the case of the main resonance with the frequency relationship $\Omega_2:\Omega_1=2:1$ takes place, where Ω_1 and Ω_2 are the imagine parts of eigenvalues. As may be inferred from the existing data, this type of resonance is of prime interest for the stellar pulsation in general and the irregular ones specifically. For this case the model (5.3) can be rearranged to the cubic approximation form

$$\frac{dc_1}{d\tau} = \sigma_1 c_1 + \Pi_1|c_2| + Q_1|c_1|^2 c_1 + T_{12}|c_2|^2 c_1$$

$$\frac{dc_2}{d\tau} = \sigma_2 c_2 + \Pi_2|c_1| + Q_2|c_2|^2 c_2 + T_{21}|c_1|^2 c_2 \qquad (5.4)$$

where c_1, c_2 are complex amplitudes of the interacting modes, $\sigma_\alpha=i\Omega_\alpha+\delta_\alpha$, $\alpha=1,2$ are the eigenvalues of the modes, $\Pi_{1,2}, Q_{1,2}, T_{12}, T_{21}$ are complex coefficients.

When studying the stellar dynamics, it was found that the resonant interaction of active ($\delta_1>0$) and passive ($\delta_2<0$) modes is the simplest and simultaneously the most typical case when chaotic pulsations come into being. We shall focus on this particular case.

Let us introducing the amplitudes a, b and phases ψ_1, ψ_2, φ in the following way

$c_1=a(\tau)\exp[i\psi_1(\tau)]$, $c_2=b(\tau)\exp[i\psi_2(\tau)]$,

$\varphi(\tau)=\psi_2(\tau)-\psi_1(\tau)-\mathrm{Im}(\Pi_2-\Pi_1)$.

Then, instead of the system (5.4), we have

$$\frac{da}{d\tau} = (\delta_1 - \delta_3 a^2)a - kab\sin\varphi$$

$$\frac{db}{d\tau} = \delta_2 b + ka^2\sin\varphi \qquad (5.5)$$

$$\frac{\varphi}{\tau} = -\Delta + \beta b^2 + k(a^2/b - 2b)\cos\varphi,$$

Here τ is the "slow" time, δ_1 and δ_2 are the real parts of the eigenvalues,

$$\Delta = 2\frac{2\Omega_1 - \Omega_2}{2\Omega_1 + \Omega_2}$$

is the detuning between eigenfrequencies Ω_1 and Ω_2; $\delta_3=\mathrm{Re}(Q_1)$, $k=\sqrt{\mathrm{Re}(\Pi_1)\mathrm{Re}(\Pi_2)}$ and $\beta=\mathrm{Im}(Q_2)$ are the coefficients describing nonlinear dissipation, resonant interaction and anharmonism, respectively. These coefficients depend in complicate way on stellar parameters.

Contrary to the usual practice of the stellar dynamics simulation (see, e.g., [45,46]), the anharmonism was taken into account in the system of equations (5.5). For simplicity sake we restrict our consideration to only one nonisochronous term

$\beta=\mathrm{Im}(Q_2)$, As it will be shown, this type of nonlinearity plays crucial role in the arising of chaotic pulsations.

5.2. Isochronous case

Let us consider first the main properties of model (5.5) for isochronous case ($\beta=0$) which was usually investigated. By solving the equations (5.5) at zero values of the time derivatives, we obtain the resonance curve which is the dependence of the stationary amplitudes A and B upon the frequency detuning Δ. All possible states of the system (4) are described by following expressions:

$$\Delta_{1,2} = \pm(\delta_2 + 2\delta_1 - 2\delta_3 A^2)\sqrt{\frac{k^2 A^2}{\delta_2(\delta_3 A^2 - \delta_1)} - 1} \tag{5.6}$$

$$B^2 = -\frac{(\delta_1 - \delta_3 A^2)^2}{\delta_2}$$

The signs "±" correspond the two independent branches of the resonant curve.

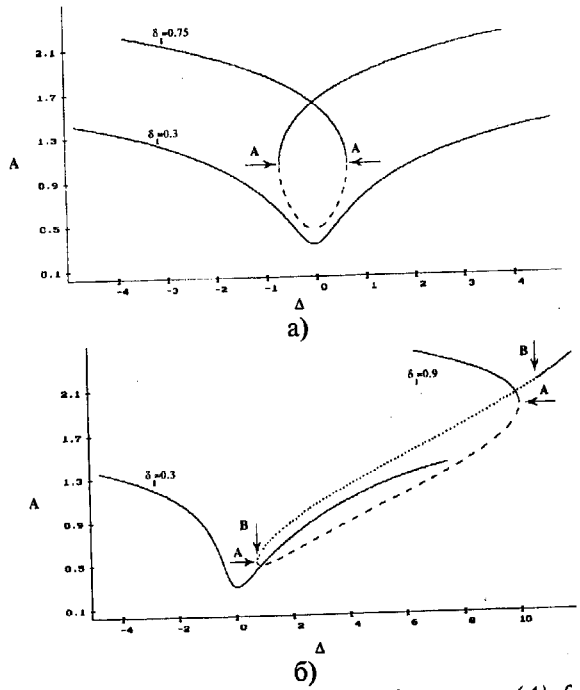

Fig.10. *The resonance curves of the system (4) for isochronous (a, $\beta=0$) and nonisochronous (b, $\beta=5$) cases and: $\delta_2=-1$, $\delta_3=0.1$, $k=2$. The letters A denotes the tangent bifurcation points, and the letters B - the Hopf bifurcation ones.*

fig 10a demonstrates the typical form of the resonance for two values of the parameter δ_1. In our calculations and analysis we used the same order parameters as in the ones, regarded previously in papers [45, 48] and characteristic of W Vir stars. In the case $\beta=0$ only the stable node-focuses (solid lines) and, when δ_1 is sufficiently large, saddle (dashed lines) stationary states may exist in the system (5.5). The latter appears when the resonance curve becomes multivalued. It indicates that the behavior of the system (4) and as well as the original hydrodynamical system (5.3) depends upon its history the system is multistable. The region of multistability is indicate by letters A on fig.1. So, there are two stable stationary states in the system, which are different in the amplitude of regular pulsations. It should be emphasize that any other regimes, excepting stationary equilibrium states that correspond to the stationary periodical regimes of the original hydrodynamical system, have not been detected for any values of the parameters. So, we may conclude that in the isochronous case the stellar dynamics is only regular.

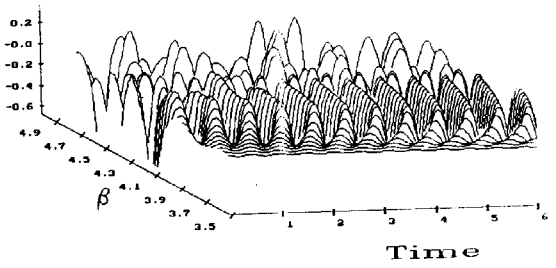

Fig.11 *The transition from regular to chaotic stellar behavior due to the variation of the parameter* β. $\delta_1=0.8$, $\delta_2=-1$, $\delta_3=0.1$, $k=2$, $\Delta=8$.

5.3. Chaotic stellar pulsations

There are theoretical and experimental evidences that the stellar oscillations possess a finite degree of anharmonism, which manifests itself through the dependence of the pulsation period versus pulsation amplitude. The decrease in star effective temperature results as a rule in the increasing of the degree of the anharmonism. It was common opinion that the effect of anharmonism is limited only by the period variations. We have found that the stellar eigenmodes anharmonism plays much more essential role in the stellar dynamics and produces not only quantitative but qualitative changes. In order to illustrate the effects of anharmonism let us refer to the results of direct simulations of system (5.5) shown on fig.11. This figure illustrates the typical evolution of the star behavior when the parameter anharmonism β is changed. Provided β is small, then the amplitude is constant in time-that corresponds to the periodic stellar pulsation. While β increases, the periodic

modulation of the amplitude appears, which corresponds to the quasiperiodic regime in the hydrodynamical stellar model. Under further β increasing the modulation becomes chaotic.

The non-zero values of stationary amplitudes A and B for the nonisochronous case can be found from the following equation of the resonance curve :

$$\Delta_{1,2} = -\frac{\beta(\delta_1 - \delta_3 A^2)^2}{\delta_2} \pm$$

$$\pm(\delta_2 + 2\delta_1 - 2\delta_3 A^2)\sqrt{\frac{k^2 A^2}{\delta_2(\delta_3 A^2 - \delta_1)} - 1} \quad , \tag{5.7}$$

$$B^2 = -\frac{(\delta_1 - \delta_3 A^2)^2}{\delta_2}$$

Its typical view is shown in fig. 10b. One can see that for small values of the parameter δ_1 describing the degree of the stellar nonequilibrium, the resonance curve is slightly different from the isochronous one. However, when δ_1 is increased, one of the stationary states in some region of the Δ variation becomes unstable, that is marked by dotted line between the points B. The different types of attractors (regular and irregular) can be formed in the phase space for this case. Consequently, the star dynamics can become extremely complicated. Let us trace the regularities of such states arising by plotting the bifurcation diagrams of regimes.

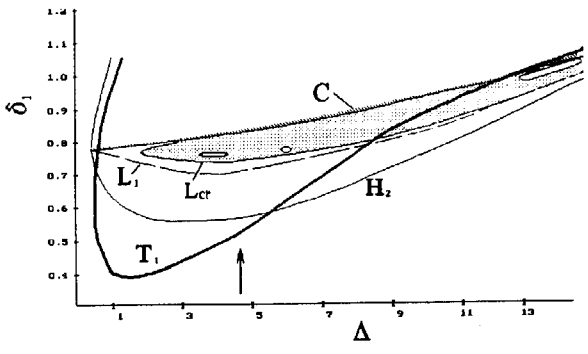

Fig.12 *The two-dimensional bifurcation diagram in the plane frequency (Δ, δ_1) for δ_2=-1, δ_3=0.1, k=2, Δ=8. The curve* ***T*** *corresponds to the tangent bifurcation,* ***C*** *- to the attractor crisis,* H_2 *- to the second Hopf bifurcation,* L_1 *- to the first doubling of the limit cycle and* L_{cr} *- to the chaos boundary.*

The two-dimensional diagram of regimes on the plane of parameters (Δ,δ_1) is shown in fig.12. It should be noted that the chaotic states exist in a narrow region of the parameter δ_1 variation and in a sufficiently wide range of the frequency detuning Δ. Now let us consider a typical transition from regular to chaotic oscillations with increasing of the parameter δ_1 in the direction marked off by the arrow in fig.12. The one-dimensional bifurcation diagram is shown in fig.13 for this case. The latter diagram is the dependence of the amplitude of the stellar pulsations versus δ_1. The increase in δ_1, as it is follow from hydrodynamical modeling [45], can be associated with the decreasing of the effective temperature T_{eff} of a star. If it is granted that the variation in T_{eff} leads to relatively small variations of other parameters of the system(5.5) then the bifurcation diagram in fig.13 displays the possible ways of the evolution of variable stars . The Hopf bifurcation is the first one which occurs when δ_1 amounts up to zero. Due to it the periodic pulsations of the star arise. Nontrivial stable solutions of the system (5.5) correspond to such states of the star. The tangent bifurcation is the next one which occurs in the system with the further δ_1 increasing The corresponding bifurcation curve is marked by T in fig.3. Two stable stationary states arise by virtue of this bifurcation. It means that the evolution of the star can take one of the two different paths, as indicated in fig.4. The specific way of the evolution is determinate by the star state at the instant before the bifurcation. It follows from the fact, that solutions of the system (5.5) depend upon the initial conditions (specific values of the mode amplitudes and phase difference). It should be emphasized that even small variations in initial conditions at this moment can radically alter the star fate. One of the ways of the star evolution may be called as the regular one (upper branch in fig.13) since on this way the regular pulsations of the star are still retained. Only quantitative variations in the amplitude of pulsations and their period are observed here.

The second way of the star evolution is more complicated. At first the system undergoes the second Hopf bifurcation (curve H_2 in fig.12), and the second independent frequency arises. As a result, the stellar pulsations become quasiperiodic with two incommensurate frequencies. It is worthy of note that from the point of view of the linear theory of the stellar pulsations only a harmonic pulsation can occur in the stellar behavior. Consequently, the second independent frequency arises due to nonlinear properties of the system.

The excitation of the quasiperiodic oscillations in the original physical system corresponds to the arising of a stable limit cycle in the phase space of the system (5.5). With the further δ_1 increasing, the destruction of the quasiperiodic oscillations through a series of the doubling bifurcations is observed. This leads to the chaotic pulsation onset.

The chaotic pulsations of the star are changed sharply to regular ones if δ_1 is large enough (see fig.13). This is conditioned by the fact that strange attractor becomes unstable and only one attracting set (stationary state on the regular branch) exists in the system (5.5). So, under large values of δ_1 the dynamics of the star is regular.

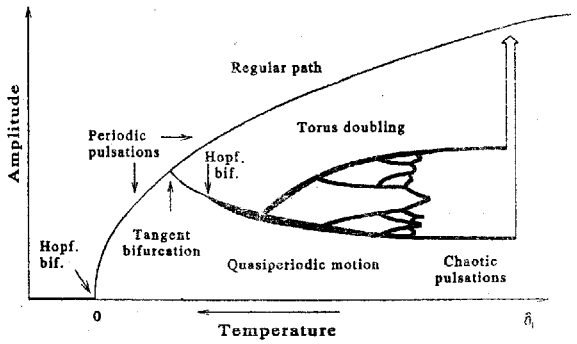

Fig.13. *The dependence of the limit cycle amplitude versus nonequilibrium parameter* δ_1.

The main results of the stellar dynamics investigation consist in following. The chaotic pulsations of W Vir stars can be described in the framework of the two-mode model. The simplicity of this model enables one to study stellar dynamics in detail. We have considered the main laws of chaos arising for the case of 2:1 resonance between these modes, however, there are good reasons to believe that these laws are the same for higher order resonances. The interaction between active and passive modes is the typical and simplest physical situation when chaotic instability arises. The main factor which is responsible for the complicate stellar dynamics is the anharmonism of the oscillating modes.

Acknowledgments

The author wishes to thank O.A.Tretyakov, A.B.Belogortsev, I.Yu.Chernyshov, V.B.Ryabov, S.A.Sharapov, and Yu.A.Tsarin for useful discussions and collaborations. This work was partly supported by the International Science Foundation (grant # U33000).

References

[1] J.Miles, Proc. Nat.Acad.Sci., Phys.Sci.USA, 81, pp.3919-3923 (1984).
[2] A.B.Belogortsev, D.M.Vavriv and O.A.Tretyakov, Sov.Phys.JETP, 65, pp.737-740 (1987).
[3] A.B.Belogortsev, D.M.Vavriv and O.A.Tretyakov, Sov.Phys.Tech. Phys, 33, pp.174- 179 (1988)
[4] K.Yagasaki, M.Sakata, and K.Kimura, ASME J. of Appl. Mech. 57, 209 (1990).
[5] K.Yagasaki, ASME Journal of Appl. Mech., 59, pp.161-167 (1992).
[6] A.B.Belogortsev, D.M.Vavriv, and O.A.Tretyakov, Appl.Mech.Rev.,46, pp.372-384 (1993).
[7] D.M.Vavriv, V.B.Ryabov, and S.A.Sharapov, Phys. Rev. E. (pending).
[8] D.M.Vavriv and I.Yu. Chernyshov, Radiotekhnika i Elektronika, 35, pp. 151-158
[9] A.B. Belogortsev, M. Poliashenko, O.A. Tretyakov, and D.M. Vavriv, Electronic Lett., 26, pp.1354-1355.
[10] A.B.Belogortsev, D.M.Vavriv and O.A.Tretyakov, Radiotekhnika i Elektronika, 35, pp.1300-1307 (1990)
[11] V.K.Melnikov, Trans. Moscow Math. Soc.12, pp. 3-57 (1963).
[12] A.D.Morosov, Diff. Equations 12, pp.164-174 (1976).
[13] P.Holmes, Philos.Trans.R.Soc.A 292, pp. 419-448 (1979).
[14] T. Kapitaniak, J. Sound Vib., 121, pp.259-265 (1988).
[15] K. Yagasaki, SIAM J. Math. Anal., 23, pp. 1230-1254 (1992).
[16] J.M.Guckenheimer and P.Holmes, Nonlinear oscillations, dynamical systems and bifurcations of vector fields (Springer, Berlin, 1983).
[17] K. Ide and S Wiggins, Physica D 34, 169 (1989).
[18] S.Wiggins, Phys.Lett.A, 124, pp. 138-142 (1987).
[19] A.B.Belogortsev, D.M.Vavriv, and B.A.Kalugin, Zh.Tekh.Fiz. 57, 559 (1987) [Sov.Phys.Tech.Phys. 32, 337 (1987)].
[20] I.Yu.Chernyshov and D.M.Vavriv, in:Proc.Int.Conf. on Noise in physical systems, Ed. A.Ambrozy (Akademiai Kiado, Budapest, 1990) p.651.
[21] N.N.Bogoliubov and Yu.A.Mitropolski, Asymptotic methods in the theory of nonlinear oscillations (Gordon & Breach, New York, 1961).
[22] V.B.Ryabov and D.M.Vavriv, Phys.Lett. A153, 431-436 (1991).
[23] D.M.Vavriv, V.B.Ryabov, and S.A.Sharapov, Radiotekhnika i Electronika, 38, pp.464-472 (1993).

[24] D.M.Vavriv and V.B.Ryabov, Dokl. Akad. Nauk UkrSSR, A2, pp.50-55 (1990).
[25] D.M.Vavriv and V.B.Ryabov, Comput. Maths & Math.Phys., 32, pp.1259-1269 (1992)
[26] A.B. Belogortsev, Nonlinearity, 5, pp.889-897 (1992).
[27] A.B. Belogortsev, Phys.Lett., A161, pp.352-356 (1992).
[28] K.Yagasaki, ASME J. of Appl. Mech. 58, pp.244-256 (1991).
[29] D.M.Vavriv, V.B.Ryabov and I.Yu.Chernyshov, Sov. Phys. Tech. Phys., 36, pp.1325-1331 (1991).
[30] D.M.Vavriv and V.B.Ryabov, Pis'ma v Zh.Tekh.Fiz. 17, pp. 55-60 (1991).
[31] I.Yu.Chernyshov and D.M.Vavriv, Phys.Lett.,A165, pp. 117-123 (1992).
[32] D.M. Vavriv, O.A.Tretyakov, I.Yu Chernyshov, Pis'ma v Zh.Tekh.Fiz.,14,pp.903-908 (1991).
[33] D.M.Vavriv and O.A.Tretyakov, Theory of Resonant Amplifiers with Distributed Interaction of O-type (Naukova Dumka Press, Kiev,1987).
[34] D.M.Vavriv and A. Oksasoglu, Electronics Lett., 30, pp. 462-463 (1994).
[35] A.Oksasoglu and D.M.Vavriv, IEEE Trans. Circuits Syst. I, 41, pp.669-672 (1994).
[36] S.A.Bulgakov, V.B. Ryabov, V.I.Shnyrkov, and D.M.Vavriv, J.Low Temp.Phys. 83 (5/6), pp. 241-255 (1991).
[37] N.F.Pedersen and A.Davidson, Appl.Phys.Lett., 39, pp. 830-836 (1981).
[38] M.Cirillo and N.F.Pedersen, Phys.Lett., A90, pp.150-157 (1982).
[39] W.C.Schieve, A.R.Bulsara, and E.W.Jacobs, Phys.Rev., A37, pp. 3541-3556 (1988).
[40] V.V.Danilov and K.K.Likharev, Radiotekhnika i Elektronika, 25, pp. 1725-1732 (1980).
[41] A.B. Belogortsev, M. Poliashenko, O.A. Tretyakov,and D.M. Vavriv, Radiotekhnika i Elektronika, 35, pp.2559-2605 (1990).
[42] D.M.Vavriv, Yu.A.Tsarin, and I.Yu.Chernyshov, Radiotekhnika i Elektronika, 36, pp. 2015-2023 (1991).
[43] A.B.Belogortsev, D.M.Vavriv and O.A.Tretyakov, Radiophys. Quantum Electron., 33, pp.187-193 (1990).
[44] A.B.Belogortsev, D.M.Vavriv and O.A.Tretyakov, Sov.Phys.Tech. Phys, 36, pp.380-385 (1991)
[45] J.R. Buchler and G. Kovacz, Astrophys. Journ.,303, pp.749-763 (1986).
[46] G. Kovacz and J.R. Buchler, Astrophys. Journ., 346, pp. 898-905 (1989).
[47] D.M.Vavriv and Yu.A.Tsarin, Kinematika i Fisika Nebesnykh Tel, 10, pp. 80-87 (1994).
[48] J.R. Buchler and G. Kovacz, Astrophys. Journ. Lett., 320, pp.57-62 (1987).
[49] P.Grassberger and I. Procaccia, Physica D, 13, pp.34-54, (1984).
[50] G. Benettin, L. Galgani, A. Giorgilli, and J.M. Strelcyn, Mechanica, 15, pp. 9-30 (1980).
[51] J.S.Nicolis, Rept. Progr. Phys. 49, pp.1109-1196 (1986).

Хаотическая динамика слабых нелинейных систем

Д.М. Ваврив

Обобщены результаты, достигнутые в последнее время при исследовании слабо нелинейных систем. Рассмотрен класс хаотических состояний, характерных для физических систем со сколь угодно слабой степенью нелинейности. Обсуждаются условия и механизмы перехода к хаосу для слабо нелинейных осцилляторов и проведено сравнение со случаем нелинейных осцилляторов. Особое внимание уделяется аналитическим методам предсказания начала хаотизации. Результаты иллюстрируются рассмотрением динамики параметрических усилителей, сквидов и переменных звезд.

Хаотична динаміка слабких нелінійних систем

Д.М. Ваврів

Узагальнено результати досліджень слабо нелінійних систем, досягнені в останній час. Розглянуто клас хоатичних станів, які характерні для фізичних систем з як завгодно слабкою ступінню нелінійності. Обговорено умови та механізми переходу до хаосу для слабо нелінійних осциляторів і проведено порівняння з сильно нелінійними осциляторами. Особливу увагу звернено на аналітичні методи передбачення початку хоатизації. Результати проілюстровано розгляданням динаміки параметричних підсилювачів,сквидів та змінних зірок.